

Ginsburg-Landau theory of solid and supersolid and their applications to ^4He

Jinwu Ye

Department of Physics, The Pennsylvania State University, University Park, PA, 16802

(Dated: December 22, 2019)

We construct a Ginsburg-Landau (GL) theory to map out the ^4He phase diagram, analyze carefully the conditions for the existence of the supersolid (SS) and study all the phases and phase transitions in a unified framework. We introduce a single parameter which is the coupling between the normal solid (NS) component and superfluid (SF) component in the GL theory. Starting from the SF side with increasing the pressure, there are two possible scenarios (1) the resulting solid is a commensurate solid (C-NS). For the first time, we derive a quantum GL action to describe the SF to the C-NS transition and explicitly derive the Feynman relation from the QGL. (2) The resulting solid is an incommensurate solid with vacancies or interstitials even at $T = 0$ whose condensation leads to the formation of a SS. The superfluid to supersolid (SS) transition is a simultaneous combination of first order transitions of superfluid density wave (SDW) formation in the superfluid sector driven by the roton condensation and NS formation in the normal density sector driven by the divergence of structure function. Then we approach the SS state from the NS side. For $g = g_v < 0$, we also find two scenarios: (1) If $|g_v|$ is sufficiently small, the C-NS is a vacancy-like NS where the excitation energy of a vacancy v is lower than that of an interstitial i , therefore named NS- v . (2) If $|g_v|$ is sufficiently large, a vacancy induced SS (SS- v) exists at sufficiently low temperature. The critical temperature T_{SS-v} becomes an effective measure of the coupling strength g . If $g = g_i > 0$, we can not get a firm conclusion, for completeness, we introduce NS- i and SS- i . For SS- v , the SDW coincides with the normal lattices, while for SS- i , the SDW takes the dual lattices of the normal lattices. The NS- v (NS- i) to the SS- v (SS- i) transition is described by a 3d XY with much narrower critical regime than the conventional NL to the SF transition. This fact is responsible for the extreme sensitivity to even tiny concentration of ^3He impurities. The X-ray scattering intensity from the SS- v is the same as that from the NS- v at mean field level, but will differ when the Dybe-Waller factor is taken into account. The X-ray scattering intensity from the SS- i ought to have an additional modulation over that of the NS- i even at mean field level. The modulation amplitude is proportional to the Non-Classical Rotational-Inertial (NCFI) observed in the torsional oscillator experiments. The X-ray scattering patterns from different lattice structures of SS- i are derived. The important effects of Dybe-Waller factor on X-ray scattering in both SS- v and SS- i are stressed. The NCFI in the SS state is calculated and found to be isotropic in bcc and fcc lattice, but weakly anisotropic in hcp lattice. All the low energy excitations in the SS phases are classified. The applications to solid hydrogen and bilayer electronic systems are briefly discussed. The analogy with type-I and type-II superconductors with g and the pressure p playing similar role as λ and the magnetic field H respectively are made. The difference and similarities with lattice supersolid are clearly demonstrated. We also make comments on other related experiments.

I. INTRODUCTION

A solid can not flow. It breaks a continuous translational symmetry into a discrete lattice translational symmetry. There are low energy lattice phonon excitations in the solid. While a superfluid can flow even through narrowest channels without any resistance. It breaks a global U(1) phase rotational symmetry and has the off-diagonal long range order (ODLRO)¹. There are low energy superfluid phonon excitations in the superfluid. A supersolid is a state which breaks both the continuous translational symmetry and the global U(1) symmetry, therefore has both the crystalline order and the ODLRO. The possibility of a supersolid phase in ^4He was theoretically speculated in 1970^{2,3,4,5}. Andreev and Lifshitz proposed the Bose-Einstein condensation of vacancies as the mechanism of the formation of supersolid². Chester wrote down a wavefunction which has both ODLRO and crystalline order and also speculated that a supersolid cannot exist without vacancies or interstitials³. Leggett proposed that solid ^4He might display Non-Classical Rotational

Inertial (NCFI) which is a low temperature reduction in the rotational moment of inertia due to the superfluid component of solid ^4He ^{4,5,6}. Leggett also suggested that quantum tunneling of He atoms between neighboring sites in a crystal can also lead to a supersolid even in the absence of vacancies. Over the last 35 years, a number of experiments have been designed to search for the supersolid state without success. However, recently, by using torsional oscillator measurement, a PSU group lead by Chan observed a marked 1–2% NCFI of solid ^4He at 0.2K, both when embedded in Vycor glass and in bulk ^4He ⁸. Some of the important experimental facts are: (1) the NCFI slides towards the normal solid regime with a very long tail. (2) the superfluid fraction has a non-monotonic dependence on the pressure, it increases first, reaches a maximum at 55 bar, then decreases to zero at a much higher pressure $p_{c2} = 170$ bar¹⁰. (3) the supersolid has a very low critical velocity corresponding to 1–3 ux quanta above which the NCFI is reduced (4) a very tiny fraction of He3 in the range of $x = 40\text{ppb} - 85\text{ppm}$ decreases the superfluid fraction

tions, but increases the supersolid to normal solid transition temperature considerably¹². This observation is very counter-intuitive and in sharp contrast to the effects of He3 impurities in both 3d ⁴He super solid and 2d super solid ⁴He in s. (5) Although the previous specific heat measurement at ³He impurities concentration $x = 30$ ppM to temperature as low as 100 mK did not detect any obvious specific heat anomaly⁹, very recent much more refined specific heat measurements in the range $x = 0.3 - 3$ ppM to temperature as low as 45 mK found a broad excessive specific heat peak around the putative supersolid onset critical temperature 100 mK¹². The authors suggested that the supersolid state of ⁴He maybe responsible for the NCFI. They mapped out the experimental global phase diagram of ⁴He in the Fig.4 in⁸. More recently, the PSU group detected about 10⁴ reduction in the rotational inertial in solid H₂¹¹, but by performing blocked cell experiments, the authors concluded that the reduction is classical due to the motion of HD impurities clustering. So the PSU group did not find any NCFI in solid hydrogen¹¹.

The PSU experiments forced us to reexamine the already fantastic physics in ⁴He and rekindled extensive both theoretical^{13,14,15,16} and experimental^{18,19,20} interests in the still controversial supersolid phase of ⁴He. There are two kinds of complementary theoretical approaches. The first is the microscopic numerical simulation¹³. The second is the phenomenological approach^{14,15,16,17}. At this moment, despite all the theoretical work, there is no consensus at all on the interpretation of PSU's experiments. A solid has the order in the number density, while a super solid has the order in the phase. The two phases are in totally different extremes of the state of matter. How to combine the two opposite extremes into a novel state of matter, supersolid, is an important and interesting topic. It is widely believed that the only chance to get a supersolid is that the solid is not perfect, namely, it is an incommensurate solid which has defects such as vacancies or interstitials, so the total number of bosons can fluctuate to give some rooms for the invasion of super solid. Due to large zero point motions, there are indeed rapid exchanging between local ⁴He atoms in bulk ⁴He, but this local process will not lead to a global phase ordering. It was estimated from both X-ray scattering experiments³⁵ and some microscopic calculations¹³ that the thermal excitation energies of a vacancy and interstitial are $v = 10$ K; $i = 40$ K, so thermal fluctuations favor vacancies over interstitials. Because both have very high energy, so the thermal generated vacancies and interstitials are irrelevant around 200 mK. However, it is still possible that there are quantum fluctuations generated vacancies and interstitials even at $T = 0$. It is still not known if quantum fluctuations favor vacancies over interstitials or not¹⁶. In this paper, we will construct a phenomenological Ginsburg Landau (GL) theory to study all the possible phases and phase transitions in helium 4 system. We identify order parameters, symmetry and symmetry breaking patterns in all

the phases. Particularly, we will address the following two questions: (1) What is the condition for the existence of the SS state? (2) If the SS exists, what are the properties of the supersolid to be tested by possible new experiments.

Let's start by reviewing all the known phases in ⁴He. The density of a normal solid (NS) is defined as $n(\mathbf{x}) = \frac{P_0}{n_0 + \int_{\mathbf{G}} n_{\mathbf{G}} e^{i\mathbf{G} \cdot \mathbf{x}}} = n_0 + n(\mathbf{x})$ where $n_{\mathbf{G}} = n_{-\mathbf{G}}$ and \mathbf{G} is any non-zero reciprocal lattice vector. In a normal liquid (NL), if the static liquid structure factor $S(\mathbf{k})$ has its first maximum peak at \mathbf{k}_n , then near \mathbf{k}_n , $S(\mathbf{k}) \sim \frac{1}{r_n + c(\mathbf{k}^2 - \mathbf{k}_n^2)^2}$. If the liquid-solid transition is weakly first order, it is known that the classical free energy to describe the NL-NS transition is^{21,28}:

$$f_n = \frac{1}{2} \frac{r_{\mathbf{G}}}{2} \int_{\mathbf{G}} \mathbf{j}_{\mathbf{G}} \cdot \mathbf{j}_{\mathbf{G}} + w \int_{\mathbf{G}_1, \mathbf{G}_2, \mathbf{G}_3} n_{\mathbf{G}_1} n_{\mathbf{G}_2} n_{\mathbf{G}_3} \mathbf{j}_{\mathbf{G}_1 + \mathbf{G}_2 + \mathbf{G}_3} + u_s \int_{\mathbf{G}_1, \mathbf{G}_2, \mathbf{G}_3, \mathbf{G}_4} n_{\mathbf{G}_1} n_{\mathbf{G}_2} n_{\mathbf{G}_3} n_{\mathbf{G}_4} \mathbf{j}_{\mathbf{G}_1 + \mathbf{G}_2 + \mathbf{G}_3 + \mathbf{G}_4} + \quad (1)$$

where $r_{\mathbf{G}} = r_n + c(G^2 - k_0^2)^2$ is the tuning parameter controlled by the pressure or temperature. Note that the average density n_0 does not enter in the free energy. Note that because the instability happens at finite wavevector, Eqn.1 is an expansion in terms of small parameter $n_{\mathbf{G}}$ alone, it is not a gradient expansion! The GL parameters w and u_s may be determined by fitting the theoretical predictions with experimental data. It is easy to see that Eqn.1 is invariant under $\mathbf{x} \rightarrow \mathbf{x} + \mathbf{a}; n(\mathbf{x}) \rightarrow n(\mathbf{x} + \mathbf{a}); n(\mathbf{G}) \rightarrow n(\mathbf{G}) e^{i\mathbf{G} \cdot \mathbf{a}}$ where \mathbf{a} is any vector. In the NL, $n(\mathbf{G}) = 0$, the translational symmetry is respected. In the NS, $n(\mathbf{G}) \neq 0$, the symmetry is broken down to translational invariance under only a lattice constant $\mathbf{a} = \mathbf{R}; \mathbf{G} \cdot \mathbf{R} = 2\pi n; n(\mathbf{x}) \rightarrow n(\mathbf{x} + \mathbf{R}); n(\mathbf{G}) \rightarrow n(\mathbf{G})$. As shown in the Fig.1, the NL to NS transition only happens at finite temperature, so the classical theory is valid. Note that due to the lack of the Z_2 symmetry of $n(\mathbf{x})$! $n(\mathbf{x})$, namely, $n_{\mathbf{G}}$, there is always a cubic w term which makes the NL to NS a 1st order transition. The u_s term which is invariant under the Z_2 symmetry is needed for the stability reason.

Of course, the Super solid to Normal Liquid transition at finite temperature in the Fig.1 is the 3d XY transition described by²⁶:

$$f = K \mathbf{j} \cdot \mathbf{j} + t \mathbf{j} \cdot \mathbf{j} + u \mathbf{j} \cdot \mathbf{j}^4 + \quad (2)$$

where K is the complex order parameter and t is the tuning parameter controlled by the temperature or pressure. Eqn.2 is invariant under the global $U(1)$ symmetry $\mathbf{j} \rightarrow e^{i\theta} \mathbf{j}$. In the NL, $\langle \mathbf{j} \cdot \mathbf{j} \rangle = 0$, the symmetry is respected. In the SF, $\langle \mathbf{j} \cdot \mathbf{j} \rangle \neq 0$, the symmetry is broken. The GL parameters K, t, u may be determined by fitting the theoretical predictions with experimental data.

The coupling between $n(\mathbf{x})$ and $\mathbf{j}(\mathbf{x})$ consistent with all the symmetry can be written down as:

$$f_{int} = g n(\mathbf{x}) \mathbf{j}(\mathbf{x}) \mathbf{j} + v (n(\mathbf{x}))^2 \mathbf{j}(\mathbf{x}) \mathbf{j} + \quad (3)$$

where $n(\mathbf{x}) = n(\mathbf{x}) - n_0 = \int_0^P n_G e^{iG \cdot \mathbf{x}} dG$. Note that the average density n_0 does not enter in the interaction either. Eqn.3 is an expansion in terms of two small parameters $n(\mathbf{x})$ and $\langle \mathbf{x} \rangle$. The terms include the other terms in higher odd and even powers of $n(\mathbf{x})$ which are sub-leading to the g and v term. In an effective GL theory, $n(\mathbf{x})$ and $\langle \mathbf{x} \rangle$ emerge as two independent order parameters. In SS-v and SS-i, $\langle \mathbf{x} \rangle$ stands for vacancies and interstitials respectively. The total density of the system is $n_t(\mathbf{x}) = n(\mathbf{x}) + j(\mathbf{x})^2$ where $n(\mathbf{x})$ is the normal density and $j(\mathbf{x})^2$ is the super uid density. This relation is straightforward for interstitials. For vacancies, if all the vacancies are in the normal state, then the solid's density is defined as $n_v(\mathbf{x})$, then the relation still holds. Eqn.3 is invariant under both the translational symmetry $\mathbf{x} \rightarrow \mathbf{x} + \mathbf{a}; n(\mathbf{x}) \rightarrow n(\mathbf{x} + \mathbf{a})$; $\langle \mathbf{x} \rangle \rightarrow \langle \mathbf{x} + \mathbf{a} \rangle$ and the global U(1) symmetry $\mathbf{x} \rightarrow e^{i\theta} \mathbf{x}; \langle \mathbf{x} \rangle \rightarrow \langle \mathbf{x} \rangle$. Note that it is important to keep both g and v term in the Eqn.3, because the g term changes the sign, while the v term is invariant under the Particle-Hole (PH) transformation

$n(\mathbf{x}) \rightarrow -n(\mathbf{x})$, so the sign of g makes a difference! Due to the two competing orders between the solid and the super uid, we expect v to be always positive and is an increasing function of the pressure p . The positive v term is also needed for the stability reason. On the other hand, we can view g as a periodic chemical potential with average zero acting on \mathbf{x} . It is easy to see the coupling is attractive $g_v < 0$ for vacancies, but repulsive $g_i > 0$ for interstitials. From Eqn.3, we can classify three kinds of solids: If $g = 0$, the C-NS has the PH symmetric C-NS as NS-PH. In general, $g \neq 0$, so there is no particle-hole symmetry in the C-NS, there are still two kinds: (1) vacancy like C-NS where the excitation energy of a vacancy is lower than that of an interstitial, named NS-v. (2) interstitial like C-NS where the excitation energy of an interstitial is lower than that of a vacancy, named NS-i. We expect that g to be an intrinsic parameter of solid Helium 4 which depends on the mass of a ^4He atom and the potential between the ^4He atoms, but not sensitive to the pressure p .

Quantum fluctuations can be incorporated by (1) $n(\mathbf{x}) \rightarrow n(\mathbf{x}; \omega)$ and including $\frac{1}{2} \nabla \cdot (\nabla n)^2$ in Eqn.1. (2) $\langle \mathbf{x} \rangle \rightarrow \langle \mathbf{x}; \omega \rangle$ and including $\langle \mathbf{x} \rangle \nabla \cdot (\nabla \langle \mathbf{x} \rangle)$ in Eqn.2. (3) Due to the lack of particle-hole symmetry in the normal solid, including additional terms like $n(\mathbf{x}; \omega) \langle \mathbf{x} \rangle \nabla \cdot (\nabla \langle \mathbf{x} \rangle)$ in Eqn.3. We will explicitly consider the quantum fluctuations in sections II and III where we will discuss super uid density wave formation in n sector only and in section IV where we will discuss the quantum phase transition from the super uid to the C-NS (either NS-v or NS-i). In the rest of the paper, we only perform our calculations at mean field level inside a given phase, then all the derivative terms can be neglected. However, they are very important to determine the low energy excitation spectra in a given phase and will be investigated in²⁹. In all the classical phase transitions addressed in this paper, we will also neglect

these quantum fluctuations. However, they are very important in the zero temperature quantum phase transition from SS-v (SS-i) to NS-v (NS-i) driven by the pressure (see Fig.2) and will be investigated in²⁹.

The GL equations 1,2,3 are invariant under both the translational symmetry $\mathbf{x} \rightarrow \mathbf{x} + \mathbf{a}; n(\mathbf{x}) \rightarrow n(\mathbf{x} + \mathbf{a})$; $n(G) \rightarrow n(G) e^{iG \cdot \mathbf{a}}$; $\langle \mathbf{x} \rangle \rightarrow \langle \mathbf{x} + \mathbf{a} \rangle$ and the global U(1) symmetry $\mathbf{x} \rightarrow e^{i\theta} \mathbf{x}; \langle \mathbf{x} \rangle \rightarrow \langle \mathbf{x} \rangle$. In a NL, $n_G = 0; \langle \mathbf{x} \rangle = 0$. In a SF, $n_G = 0; \langle \mathbf{x} \rangle \neq 0$. In a NS, $n_G \neq 0; \langle \mathbf{x} \rangle = 0$, while in a supersolid, $n_G \neq 0; \langle \mathbf{x} \rangle \neq 0$. From the normal liquid (NL) side, one can approach both the solid and the super uid. Inside the NL, $t > 0$, has a gap, so can be integrated out from Eqn.3, we recover the solid-liquid transition tuned by r_G in Eqn.1 (Fig.2). Inside the NL, $\langle n(\mathbf{x}) \rangle = n_0$, the density fluctuations of $n(\mathbf{x})$ is massive, so can be integrated out from Eqn.3, then we recover the NL to SF transition tuned by t in Eqn.2 (Fig.1).

Although the NL-NS and NL-SF transitions are well understood, so far, the SF-NS transition has not been investigated seriously. This transition may be in a completely different universality class than the NL-NS transition, because both sides break two completely different symmetry: internal global U(1) symmetry and translational (and orientational) symmetry. It is possible that the solid reached from the SF side is a new kind of solid than the NS reached from the NL side. In a recent paper²³, we constructed a simple, novel and powerful two components quantum Ginsburg Landau (QGL) theory in the n sector to study super uid density wave formation transitions in the super uid. As shown in²³, the problem of studying super uid density wave formation inside a super uid state is interesting on its own. In this paper, using the QGL theory developed in²³ and incorporating the couplings g and v between n and $\langle \mathbf{x} \rangle$ sector in Eqn.3, we determine the global¹⁴ phase diagram and study all the phases and phase transitions in a unified framework. Starting from the SF side with increasing pressure, we develop the theory based on the two facts (1) there is a roton minimum in the super uid state (2) The instability to solid formation is driven by the gap diminishing at the roton minimum. The fact (1) was well established. The fact (2) also has some earlier theoretical and experimental supports (see^{24,25} and references therein). As shown in this paper, the fact (2) is guaranteed by the Feynman relation Eqn.10 which relates the roton minimum to the peak of the structure factor. The resulting solid at high pressure could be an incommensurate solid with zero point quantum fluctuations generated vacancies or interstitials whose condensation leads to the formation of the SS-v and SS-i respectively (Fig.2). Starting from the NS side, we show that the local tunneling processes in the NS-PH only leads to local fluctuations of n with a gap (ρ) in Fig.3, so there is no long-range phase coherence and no supersolid in this case $T_{ss} = 0$. Taking the NS-PH state as the reference state, we will show that if the coupling in Eqn.3 is sufficiently negative (or positive), the supersolids SS-v or SS-i can be realized by

adding small number of vacancies to N S-v or interstitials to the N S-i (Fig 3). The attractive (repulsive) interaction is shown to be crucial to raise the normal solid to the vacancy (interstitial) induced supersolid transition temperature $T_{SS\text{-}v}$ ($T_{SS\text{-}i}$) above the zero temperature in the Fig 3. In fact, the temperature T_{SS} becomes an effective measure of the coupling strength g . This paper will explore many important physical consequences due to this single coupling g . In section V I, we find that SS-v is more likely than SS-i. However, in order to be complete, we study both cases on the same footing. It is also constructive to compare SS-v with SS-i even though the SS-i is unlikely to be relevant to the Helium 4 system. We call vacancies induced supersolid as SS-v, interstitials induced supersolid as SS-i. When the two kinds of SS show different properties, we treat them differently, when they share the same properties, we treat them just in the same notation SS. The SS phase naturally and consistently fits into the phase diagram. The theory can be used to address several important phenomena observed in the P SU experiments and also make sharp predictions to be tested by possible future experiments, especially X-ray scattering experiments in the SS state. Our main results on supersolid are independent of many microscopic details, should be universal and may have some applications on P SU's experiments on ^4He and other systems.

The rest of the paper is organized as the following: In Sec. II, we rephrase the two component Q GL theory in the sector developed in²³ using ^4He superuid notations. In Sec. III, we use the Q GL theory to study the superuid to superuid density wave (SDW) transition driven by the roton condensation at $k = k_r$ in the sector alone which is interesting on its own. In Sec. IV, for the first time, we construct a quantum Ginsburg-Landau action to study SF to the NS transition and also explicitly establish the Feynman relation from the Q GL. In Sec. V, taking into account the couplings between the n and sector encoded in Eqn 3, we study the superuid to supersolid transition which is a simultaneous combination of the SDW transition in sector driven by the roton condensation at $k_0 = k_r$ discussed in Sec. III and the NS transition in the n sector driven by the divergence of the structure function at $k_0 = k_r = k_n$ discussed in Sec. IV. We also sketch the global phase diagrams to be confirmed and analyzed in the following sections. In Sec. VI, we approach the SS phase from the NS side and discuss the SDW in SS-v and SS-i respectively. We analyze carefully the conditions for the existence of SS-v. We explicitly show that the SS-v is the possible ground state when the g_v is sufficiently negative (Fig 3). The SS-i is unlikely, but we still analyze SS-i in the same footing as SS-v. We also classify several common SS-i lattice structures. In Sec. VII, we make key predictions on the elastic X-ray scattering amplitudes from all SS-v and SS-i structures classified in Sec. VI. These predictions are amenable to ongoing X-ray scattering experiments at P SU¹². In Sec. VIII, we calculate the NCRIs in both the SF and SS states and find the NCRi in the hcp SS lattice may be

weakly anisotropic. In Sec. IX, we discuss all the low energy excitations in the SS state and also estimate the very large vortex size and low critical velocity in the supersolid state. In Sec. X, we compare the properties of the SS with those of lattice SS on extended boson Hubbard model. In Sec. XI, we apply our theory to analyze the P SU's experiments in ^4He , especially the dramatic effects of He3 impurities and also comment on several other experiments. The applications of the GL theory on Hydrogen and fermionic systems such as bilayer quantum Hall systems and electron-hole bilayer systems are also briefly mentioned. Analogy with Type-I and Type-II superconductors are made. Conclusions are summarized in the final section XII. In the appendix, we discuss the properties of a tight-binding toy SS-v wavefunction. A short report of these results appeared in¹⁷ where only the X-ray scattering from SS-i is emphasized.

II. TWO-COMPONENT Q GL THEORY IN THE SECTOR

The superuid is described by a complex order parameter whose condensation leads to the Landau's quasi-particles. Although the bare ^4He atoms are strongly interacting, the Landau's quasi-particles are weakly interacting. Usually, ϕ describes fluctuations near $k = 0$, while a superuid density wave (SDW) is described by a density operator which sets up a lattice scale at $k = 1/a$ where a is the lattice constant. In order to describe both superuid and superuid density wave on the same footing by a Q GL theory, we will take the ϕ as the primary order parameter, while the superuid density operator

$= j \dot{\phi}$ just as a descendent (or derivative) order parameter. Note that ϕ is different from $n(x)$ in Eqn 1 which should be taken as an independent variable in the effective GL theory. This indicates that the resulting SDW not only has the conventional translational and rotational orders characterized by ϕ , also has a quantum phase order characterized by the more fundamental order parameter ϕ . The most general Quantum Ginsburg-Landau (Q GL) action at any dimension, any pressure and any temperature to supersede Eqn 2 is:

$$S = \frac{1}{2} \int d^d x d [\frac{1}{2} \dot{\phi}^2 + \frac{1}{2} \dot{\phi}^2 + t \dot{\phi}^2 + K \dot{\phi}^2 + L_1 \dot{\phi}^2 + L_2 \dot{\phi}^2] + u \int d^d x d j(x; \phi)^4 + \dots \quad (4)$$

In the following, for simplicity, we neglect the linear derivative terms, so the sector has the P-H symmetry. However, main physics in the sector stays the same if this term is included, therefore, the P-H symmetry is removed.

The above equation generalize Eqn 2 to include the strong long-range interaction between ^4He atoms which are incorporated into $L_1; L_2$ terms, the residue short-range interaction u is weak, so a perturbative expansion in terms of u is possible. The hard core and long-

range Lennard-Jones potential between ${}^4\text{He}$ atom's lead to $L_1 < 0; L_2 > 0$ in the super uid state where $t < 0$. This fact, in turn, leads to the dispersion curve of super uid state $!^2 = K q^2 - L_1 j_1^4 + L_2 q^6$ (see also Eqn.13) shown in Fig. 1 b which has both a phonon sector and a roton sector. In order to focus on the low energy modes, we divide the spectrum into two regimes: the low momenta regime $k < k_r$ where there are phonon excitations with linear dispersion and high momentum regime $j_1 k_r < k < k_r$ where there is a roton minimum at the roton surface $k = k_r$. We separate the complex order parameters $(\mathbf{x}; \mathbf{k}) = j_1(\mathbf{x}; \mathbf{k}) + j_2(\mathbf{x}; \mathbf{k})$ into $j_1(\mathbf{x}; \mathbf{k}) = \int_0^{\frac{d^d k}{(2)^d}} e^{i\mathbf{k} \cdot \mathbf{x}} j_1(\mathbf{k}; \mathbf{x})$ and $j_2(\mathbf{x}; \mathbf{k}) = R \int_{k_r}^{\frac{d^d k}{(2)^d}} e^{i\mathbf{k} \cdot \mathbf{x}} j_2(\mathbf{k}; \mathbf{x})$ which stand for low energy modes near the origin and k_r respectively. For the notation simplicity, in the following, \mathbf{m} means $j_1 k_r j_2$.

The GL action in the $(\mathbf{x}; \mathbf{k})$ space becomes:

$$\begin{aligned} S = & \frac{1}{2} \int_0^Z \frac{d^d k}{(2)^d} \int_{i!_n}^X (-!_n^2 + t + K k^2) j_1(\mathbf{k}; \mathbf{x}) j_1^2 \\ & + \frac{1}{2} \int_0^Z \frac{d^d k}{(2)^d} \int_{i!_n}^X (-!_n^2 + r + v_r (k - k_r)^2) j_2(\mathbf{k}; \mathbf{x}) j_2^2 \\ & + u \int d^d x d^d \mathbf{k} j_1(\mathbf{x}; \mathbf{k}) + j_2(\mathbf{x}; \mathbf{k})^2 \end{aligned}$$

where t is the compressibility, $r = T - T_c$ where $T_c = 2.17\text{K}$ is the critical temperature of super uid to normal uid transition at $p = 0.05\text{ bar}$ and $r = p - p_{c1}$ where $p_{c1} = 25\text{ bar}$ is the critical pressure of super uid to the supersolid transition at $T = 0$.

The fact that the spectrum in the super uid state has low energy modes at two different momentum regimes originates from the strong interactions between ${}^4\text{He}$ atom's. It is this salient feature which is at the heart of the possible formation of the state of supersolid to be discussed in the following section. At the starting point, we have only one complex order parameter j . However, due to this unique feature, it splits into two complex order parameters j_1 and j_2 which represent the two low energy modes at the origin and k_r respectively. The coupling between the two modes is naturally encoded in the quartic u term in Eqn.5. Note that despite this splitting, there is only one $U(1)$ global symmetry $j_1 \neq 0; j_2 \neq 0$. It also has only one Particle-Hole (PH) symmetry $j_1 \neq 0; j_2 = 0$. In principle, the PH symmetry breaking terms like γ_0 may exist, but they are irrelevant in the SF phase. In conventional cases, "hard" spin model is equivalent to "soft" spin model in the long wavelength limit. However, in the presence of the low energy mode j_2 at a finite roton wavevector $k = k_r$, the two models may not be equivalent anymore. Our "soft" spin model Eqn.5 puts the fluctuations of j_1 and j_2 on the same footing, therefore has the advantage over a "hard" spin model where there is only phase fluctuations.

III. SUPERFLUID TO SUPERFLUID DENSITY WAVE (SDW) TRANSITION IN THE SECTOR

In this section, neglecting the coupling between the n sector and the σ sector in Eqn.3, we apply the results on the super uid to super uid density wave transition in σ sector achieved in detail in²³ specifically to ${}^4\text{He}$ super uid. In section V, restoring the coupling, we will study the SF to SS transition in the complete QGL action Eqns.1,5,3.

In the super uid state, $t < 0; r > 0$, so j_1 develops a non-vanishing expectation value $\langle j_1 \rangle = a \neq 0$. As one increases the pressure p , the interaction u also gets bigger and bigger, the roton minimum gets deeper and deeper,

r gets smaller and smaller as demonstrated by inelastic neutron scattering of super uid ${}^4\text{He}$ ^{24,25}. At mean field level treatment of j_1 , simply setting $j_1(\mathbf{x}; \mathbf{k}) = a^2$ into the interaction term in Eqn.5, we find the interaction term becomes:

$$\begin{aligned} V(j_1 = a; j_2) = & u [a^4 + j_2^4 + 2a^2 j_2 j_2^2 + 4a^2 (R e_2)^2 \\ & + 4a^3 R e_2 + 4a j_2 j_2^2 R e_2] \end{aligned} \quad (6)$$

Obviously, the condensation of j_1 breaks the $U(1)$ symmetry of j_2 . This is expected, as stressed previously, there is only one $U(1)$ symmetry anyway. The linear term⁵ in j_2 in Eqn.6 vanishes, because $\int d^d x R e_2(\mathbf{x}; \mathbf{k}) = R e_2(\mathbf{k} = 0; \mathbf{x}) = 0$. Because the $U(1)$ symmetry of j_2 is already broken, it is convenient to separate j_2 into real and imaginary parts $j_2(\mathbf{x}; \mathbf{k}) = j_1(\mathbf{x}; \mathbf{k}) + i j_2(\mathbf{x}; \mathbf{k})$, the action inside the SF state is:

$$\begin{aligned} S_{sf} = & \frac{1}{2} \int_0^Z \frac{d^d k}{(2)^d} \int_{i!_n}^X (-!_n^2 + (r + 6ua^2) + v_r (k - k_r)^2) j_1 j_1^2 \\ & + \frac{1}{2} \int_0^Z \frac{d^d k}{(2)^d} \int_{i!_n}^X (-!_n^2 + (r + 2ua^2) + v_r (k - k_r)^2) j_2 j_2^2 \\ & + u \int d^d x \int d^d \mathbf{k} [(j_1^2 + j_2^2)^2 + 4a^3 j_1 j_2^2] \end{aligned} \quad (7)$$

Because the particle-hole (PH) symmetry $j_2 \neq 0$ remains unbroken, the Z_2 symmetry $j_2 \neq 0$ remains. Obviously, j_1 is more massive than j_2 , therefore can be integrated out. Finally, we reach the following $n = 1$ component $(d; d_2) = (d + 1; d)$ quantum Lifshitz (QLF) action²⁸ to describe super uid to the super uid density wave (SDW) transition:

$$\begin{aligned} S_{sf} = & \frac{1}{2} \int_0^Z \frac{d^d k}{(2)^d} \int_{i!_n}^X (-!_n^2 + j_2 r + v_r (k - k_r)^2) j_2 j_2^2 \\ & + u \int d^d x \int d^d \mathbf{k} j_2^4 + \end{aligned} \quad (8)$$

where $u > 0$, $r = p - p_{c1}$ is the renormalized mass, $p_{c1} = 25\text{ bar}$ is the critical pressure of the SF to the SDW transition, γ_0 stands for possible high power terms like $u_{2m}^2 j_2^m$ and j_2^3 . Note that there is no 3rd power terms like j_2^3 due to the Z_2 symmetry of j_2 . When

$\omega_r > 0$, $\langle \omega_r \rangle = 0$, the system is in the SF phase. When $\omega_r < 0$, it is in a super uid density wave phase where $\langle \omega_r \rangle$ takes a lattice structure $\langle \omega_r(\mathbf{x}) \rangle = e^{i\omega_r} \sum_{m=1}^p e^{iQ_m} \times$ where Q_m is a uniform globalphase and $Q_m = \mathbf{k}_r; m = 1; \dots, p$; ³⁰ The lattice structure with lattice constant $a = 1/k_r$ can be determined by a energy minimization which depends on microscopic details. Because $u > 0$, at mean field level, there is a 2nd order SF to SDW transition at $\omega_r = 0$. This is in sharp contrast to the conventional liquid-solid transition described by Eqn.1 which is 1st-order transition even at the mean field level due to the presence of a 3rd power term. In ³¹, Shankar developed a Renormalization Group (RG) analysis to study the stability of Fermi surface under the interactions between fermions. In this RG, the scalings are performed around the Fermi surface where there are low energy excitations. Because there are low energy excitations around the roton surface, it is tempting to apply Shankar's method to study the effects of fluctuations around the roton surface. For simplicity, we only consider classical phase transitions at finite T , so we set $\langle n \rangle = 0$ in Eqn.8. Making shift $\mathbf{k} \rightarrow \mathbf{k} + \mathbf{k}_r$ in the Q-LF action Eqn.8, we can rewrite the action Eqn.8 as:

$$S_{\text{sf}} = \frac{1}{2} \int \frac{d\mathbf{k}}{2} \int d\omega (\omega_r + v_r k^2) j_2(\mathbf{k}; \omega) j_2(\mathbf{k}; \omega) + u \int \frac{Y^3}{2} \int \frac{d\mathbf{k}_i}{2} \int d\omega j_2(\mathbf{k}_1; \omega) j_2(\mathbf{k}_2; \omega) j_2(\mathbf{k}_3; \omega) j_2(\mathbf{k}_4; \omega) +$$

where momentum conservation is assumed in the interaction u term and Y is the solid angle in dimension. Following Shankar, we integrate out the high energy modes with $|j_2| = b$, keep the low energy modes at $|j_2| = b$. Then rescale $k^0 = bk$ and normalize the ω field such that to keep the v_r term invariant. We find the recursion relations $\omega_r^0 = b^2 \omega_r$; $u^0 = b^3 u$. In fact, $u_{2m}^0 = b^{m+1} u_{2m}$ for any m . So all the possible interaction terms are relevant. It indicates that the SF-SDW transition is always fluctuation driven 1st order. This RG analysis confirms the original picture in ³². This is in sharp contrast to the interacting fermions where only the quartic term u is marginally relevant (irrelevant) if it is positive (negative), while high power terms like u^{2m} ; $m > 3$ are irrelevant.

IV. SUPERFLUID TO NORMAL SOLID TRANSITION

In the last section, we studied the SF to SDW transition in the ω sector. In this section, we will study the SF to the NS transition. In the super uid state, if the multi-quasiparticle part can be neglected in the dynamical structure factor, the Feynman relation between the Landau quasi-particle dispersion relation in the ω sector and

the static structure factor in the n sector holds:

$$S(\mathbf{q}) = \frac{q^2}{2m S(\mathbf{q})} \quad (10)$$

In the $q \rightarrow 0$ limit, $S(\mathbf{q}) \propto q$, $S(\mathbf{q}) \propto q^2$ recovers the super uid phonon spectrum near $q = 0$ in the ω sector. The first maximum peak in $S(\mathbf{q})$ corresponds to the roton minimum in $S(\mathbf{q})$ in the ω sector (Fig.1b), namely, $k_n = k_r$. As one increases the pressure p , the interaction u also gets bigger and bigger, the first maximum peak of $S(\mathbf{q})$ increases, the roton minimum k_r gets smaller and smaller²⁴. Across the critical pressure $p = p_c$, there are the two possibilities. (1) The resulting solid is a commensurate solid, then $\langle n \rangle = 0$. In the NS, there is no remnant of the roton inside the SF, the supersolid phase does not exist as an equilibrium ground state. This is the SF to the CS transition. In section VI, this happens when gj is sufficiently small (Fig.1). (2) The resulting solid at high pressure is an incommensurate solid with zero point quantum fluctuations generated vacancies or interstitials whose condensation leads to the formation of the SS-v and SS-i respectively. In section VI, this happens when gj is sufficiently large (Fig.2). We will discuss case (1) in this section, then the most interesting case (2) in the next section.

The effective action inside the SF is:

$$L[n] = i n \partial_\omega + \frac{1}{2} s(r) \omega^2 + \frac{1}{2} n V_n(\mathbf{q}) n \quad (11)$$

where s is the super uid density and $V_n(\mathbf{q}) = a - b\mathbf{q}^2 + c\mathbf{q}^4$ with $a > 0$; $b > 0$ is the density-density interaction between the ${}^4\text{He}$ atoms.

In the SF state, it is convenient to integrate out n in favor of the phase field to get the phase representation

$$L[n] = \frac{1}{2V_n(\mathbf{q})} (\partial_\omega)^2 + \frac{1}{2} s(r) \omega^2 \quad (12)$$

where the dispersion relation of the super uid modes including higher orders of momentum can be extracted³⁴:

$$\omega^2 = [s V_n(\mathbf{q})] \mathbf{q}^2 = 2 s \mathbf{q}^2 (a - b\mathbf{q}^2 + c\mathbf{q}^4) \quad (13)$$

It is easy to see that the dispersion relation indeed has the form shown in Fig.1b with a roton minimum. Because the original instability comes from the density-density interaction $V_n(\mathbf{q})$, it is convenient to integrate out the phase field in favor of the density fluctuation operator n . Neglecting the vortex excitations in and integrating out the n in Eqn.11 leads to:

$$L[n] = \frac{1}{2} n \left(\partial_\omega \right) \left[\frac{\omega^2}{s \mathbf{q}^2} + V_n(\mathbf{q}) \right] n(\mathbf{q}; \omega) \quad (14)$$

where we can identify the dynamical pseudo-spin density-density correlation function $S_n(\mathbf{q}; \omega) = \langle n(\mathbf{q}; \omega) n(\mathbf{q}; \omega) \rangle = \frac{s \mathbf{q}^2}{\omega^2 + V_n(\mathbf{q}) \mathbf{q}^2}$ where $V^2(\mathbf{q}) = s V_n(\mathbf{q})$ is the spin wave velocity.

From the pole of the dynamic density-density correlation function, we can identify the speed of sound wave which is exactly the same as the spin wave velocity. This should be expected. From the analytical continuation $i!_n \rightarrow -i$, we can identify the dynamic structure factor: $S_n(q; !) = S_n(q) (1 - v(q)q)$ where $S_n(q) = s q = 2v(q)$ is the equaltime density correlation function shown in Fig.1b. As $q \rightarrow 0$, $S_n(q) \propto q$. The Feynman relation which relates the dispersion relation to the equaltime structure factor is:

$$!_n(q) = \frac{s q^2}{2S_n(q)} \quad (15)$$

which takes exactly the same form as Eqn.10 if we identify $s = 1 = m$ with m the mass of ^4He mass. Therefore, we recovered the Feynman relation from our GL theory Eqn.11 which gives us the confidence that Eqn.11 is the correct starting action to study the SF to SS transition. The density representation Eqn.14 is dual to the phase representation Eqn.12. However, the phase representation Eqn.12 contains explicitly the superuid order parameter ϵ which can be used to characterize the superuid order in the SF phase. While in Eqn.14, the signature of the superuid phonon mode is encoded in the density sound mode, because the order parameter is integrated out, the superuid order is hidden, so it is not as powerful as the phase representation in describing the SF state. However, as shown in the following, when describing the transition from the ES to the NS, the density representation Eqn.14 has a big advantage over the phase representation.

Because the instability is happening at $q = q_0$ instead of at $q = 0$, the vortex excitations remain uncritical through the SF to SS transition. Integrating them out will generate interactions among the density n :

$$L[n] = \frac{1}{2} n(\mathbf{q}; \mathbf{k}) \left[\frac{!_n^2}{s q^2} + V_n(\mathbf{q}) \right] n(\mathbf{q}; !_n) \\ w(n^3 + u(n^4))$$

where the momentum and frequency conservation in the quartic term is assumed. Note that the $(!_n = q)^2$ term in the first term stands for the quantum fluctuations of n which is absent in the classical NL to NS transition Eqn.1. Because of the lack of Z_2 exchange symmetry, there is a cubic term in Eqn.17. Expanding $V_n(\mathbf{q})$ near the roton minimum q_0 leads to the quantum Ginsburg-Landau action to describe the SF to the NS transition:

$$L[n] = \frac{1}{2} n A_n !_n^2 + r + c(q^2 - q_0^2) n \\ w(n^3 + u(n^4)) \quad (17)$$

where $r = R_1$, p and $A_n = \frac{1}{s q_0^2}$ which is non-critical across the transition. Just like Eqn.1, because the instability happens at the finite wavevector $q = q_0$, Eqn.17 is not a gradient expansion, but an expansion in terms of the small order parameter n . Again the average density

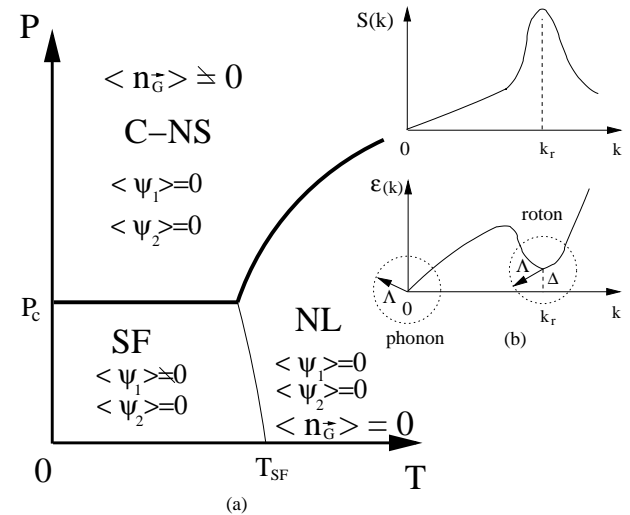


FIG. 1: (a) The theoretical phase diagram of GL model Eqns.1,2 and 5 in P versus T plane. This phase diagram only happens when $!_n$ is sufficiently small, so the normal solid is a C-NS (Fig.3). T controls thermal fluctuations, while P tunes quantum fluctuations. SF is the superuid phase, C-NS is the commensurate normal solid phase which still does not have the P-H symmetry, it is likely to be a vacancy-like C-NS (NS-v). NL is the normal liquid phase. The supersolid phase is absent. Thick (thin) lines are 1st (2nd) order transitions. The critical temperatures T_{SF} of NL to SF transition drops slightly as the pressure P increases because of the quantum fluctuations. The SF to the C-NS transition is described by the QGL Eqn.17. (b) The structure factor and the separation of low (phonon) and high (roton) momentum regime in the dispersion relation in the SF. The Feynman relation between the two curves are explicitly derived in Eqn.15.

n_0 does not appear in Eqn.17. The generic transition driven by the collapsing of roton minimum is from SF to NS instead of from the SF to the supersolid (SS). In the SF, $r > 0$; $\epsilon > 0$; $\langle n \rangle = 0$. In the NS, $r < 0$; $\epsilon = 0$; $\langle n \rangle = \int_{\mathbf{G}} n_{\mathbf{G}} e^{i\mathbf{G} \cdot \mathbf{k}}$ where \mathbf{G} are the shortest reciprocal lattice vector of the resulting lattice.

The corresponding phase diagram for the SF to the NS transition is shown in Fig.1.

In the Fig.1, even the SS does not exist as an equilibrium state, it may still exist as a metastable state which is interesting on its own, because it may have important observable effects which will be discussed in Section IX. A similar 2+1 dimensional zero temperature excitonic superuid to pseudo-spin density wave (PSDW) transition in bilayer quantum Hall system was worked out in⁵².

V. SUPERFLUID TO SUPERSOLID TRANSITION AND GLOBAL PHASE DIAGRAM

In the last two sections, we discuss the SF to the PSDW transition with the order parameter n and the SF to the

NS transition with the order parameter n respectively. In this section, we discuss the SF to the SS transition with both order parameters and n . Then we have to also include the couplings between n and n sector encoded in Eqn.3. As pointed out in²³, the most difficult uncertainty in the SF-SDW transition is to determine the lattice structure of the SDW in the sector which depends on microscopic details. Very fortunately, as shown in this section, this uncertainty disappears when the couplings Eqn.3 are taken into account, the SF to SDW transition in the sector becomes a SF to SS transition in the ^4He system.

Across the phase boundary $p = p_{c1}$ in Fig.2, the resulting solid could be an incommensurate solid (IC-NS) with vacancies or interstitials even at $T = 0$ whose condensation leads to $\langle n \rangle \neq 0$ ^{2,3,16}. There is still some remnant of the SF in the IC-NS, the supersolid phase does exist as an equilibrium ground state. In this section, we assume g_{ij} is sufficiently large in Fig.2 and study the SF to the SS transition across $p = p_{c1}$. Because n is also critical through the transition, we can not simply integrate it out like in the last section. In fact, in the effective GL theory, we have to treat n and n on the same footing. From Eqn.1 and Eqn.5, we can see that n and n have very similar propagators, so the lattice formation in n sector with $n(x) = n_0 + \sum_{G \neq 0} n_G e^{iG \cdot x}$ where $G = k_n$ and the superfluid density wave (SDW) formation in n sector with $\langle n_2(x) \rangle = \sum_{m=1}^P e^{iQ_m \cdot x}$ where $Q_m = k_r = k_n$ have to happen simultaneously. From Hansen-Verlet criterion²⁸, when $S(k_r) = n_0$ is sufficiently large, solidification in the n sector occurs, so the roton minimum remains finite just before its condensation. So strictly speaking, the RG analysis in Eqn.9 holds only in the absence of the n coupling. The SDW $= j_1 + j_2$ is simply locked to (or commensurate with) the underlying normal solid (n) lattice. In fact, this locking is dictated by the density- n density couplings in Eqn.3. If the coupling g is attractive $g_v < 0$, the SDW just coincides with the n lattice. If it is repulsive $g_v > 0$, then it simply shifts the SDW by suitable constants along the three unit vectors in the direct lattice. These constants will be determined in the next section for different n lattices. Namely, the supersolid states consist of two interpenetrating lattices formed by the n lattice and the n superfluid density wave. In fact, in a carefully prepared super-pressured sample, the roton minimum survives up to a high pressure as $p_r = 120$ bar. This fact suggests the roton minimum in the meta-stable state in a super-pressured sample is replaced by a SDW which is commensurate with the n lattice in the stable SS state. Strikingly, this pressure $p_r = 120$ bar is close to $p_{c2} = 170$ bar in Fig.2 where the NCR was extrapolated to vanish in the PSU's experiments¹⁰. This consistency also leads some support to the above picture. Obviously, when the pressure is so high that $p > p_{c2}$ in Fig.2, C-NS is the only possible ground state, any remnant of the SF completely disappears. So the vertical axis in the Fig.2 shows the SF-SS-NS series as the pressure P increases at

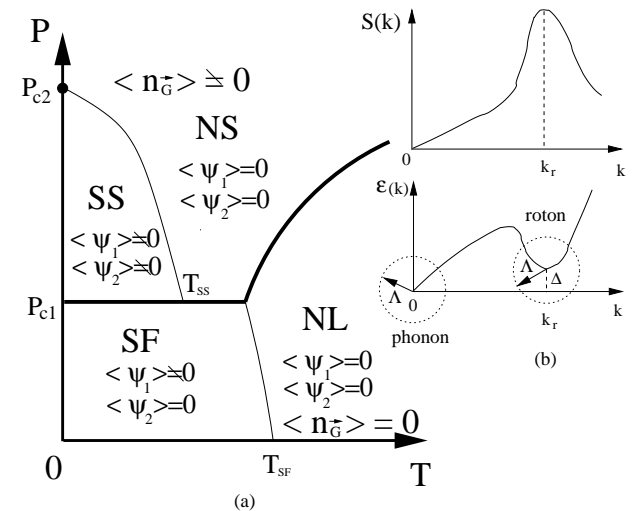


FIG. 2: (a) The theoretical phase diagram of GL model Eqsns.1,2 and 5 in the pressure P versus temperature T plane. This phase diagram only happens when g_{ij} is sufficiently large (Fig.3). T controls thermal fluctuations, while p tunes quantum fluctuations. SF is the superfluid phase, NS is the normal solid phase, it is likely to be a vacancy-like normal solid (NS-v). NL is the normal liquid phase. The SS is likely to be the vacancies induced supersolid (SS-v). T_{ss} is an effective measurement of the strength of the coupling constant $g \neq 0$ in Eqn.3. Thick (thin) lines are 1st (2nd) order transitions. The critical temperatures of NL to SF and NS to SS transitions drop slightly as the pressure p increases because of the quantum fluctuations. The SF to the SS transition is a simultaneous combination of the SDW transition in sector driven by the roton condensation at $k_0 = k_r$ and the NS transition in the n sector driven by the divergence of the structure function at $k_0 = k_r = k_n$. (b) The structure factor and the separation of low (phonon) and high (roton) momentum regime in the SF.

$T = 0$

Combining the roton condensation picture³³ in the last section with the results reviewed in the introduction, we can sketch the following phase diagram Fig.2 of the complete GL Eqsns. 1, 5 and 3.

As can be seen from the Fig.2, starting from the SF side, as the pressure is increased at a given temperature, there are two possible states (1) At very low $T < T_{ss}$, the Bose-Einstein condensation (BEC) of n_2 leads to the supersolid state where $\langle n_1 \rangle = 0$; $\langle n_2 \rangle \neq 0$; $\langle n_G \rangle \neq 0$. The instability happens at a finite wavevector $k = k_r$ instead of at $k = 0$. (2) At higher temperature $T_{ss} < T < T_{sf}$, there is a direct SF to NS transition. The SS state is certainly different from a conventional normal solid phase where $\langle n_1 \rangle = \langle n_2 \rangle = 0$; $\langle n_G \rangle \neq 0$. In addition to the conventional translational and rotational orders characterized by n (which is the same as those characterized by n), the SS also has the ODLRO characterized by n_1 and n_2 . When decreasing the temperature at a given pressure, if $p < p_c$, the NL becomes SF at

$T = T_{SF}$, the instability happens at $k = 0$. If $p > p_c$, the NL becomes a NS first at $T = T_m$, then there is a SDW onset transition from the NS to a SS phase at $T = T_{SS}$. Starting from $T = 0$ and increasing the temperature, if $p < p_c$, the transition from the SF to the NL is driven by vortex unbindings; if $p > p_c$, the transition from the SS to the NS is also driven by the vortex unbinding in the globalphase 2 (see Eqn 24), the phonon modes in the SS are non-critical across the transition, as the temperature increases further, the phonon modes drive the melting of the NS into the NL.

Because the SF to SS transition driven by the roton condensation can be either weakly or strong first order, in principle, Eqs. 8, 17 work precisely only in the SF side, it is not easy to study the precise nature of the SS state from the SF side. It turns out that it is more convenient to study the properties of the SS state from the NS side in the next section. The results achieved from the NS side in the following section indeed confirm the roton condensation picture and the globalphase diagram Fig. 1.

VI. THE NORMAL SOLID TO THE SUPER SOLID TRANSITION

In this section, we approach the SS phase from the normal solid side and confirm it indeed exists and determine its lattice structure. In the NL to the SF transition at $T = T_{XY} = 2.17K$, the BEC happens in the 1 sector at $k = 0$, 2 has a large gap and can be simply integrated out. In the NS, v stands for the vacancies or interstitials coming from the large zero point quantum fluctuations^{2,3,16}. Inside the NS, the translational symmetry is already broken, we can simply set $n(\mathbf{x}) = n(\mathbf{x})$ $\eta_0 = \frac{P}{G} \int_0^0 n_G e^{iG \cdot \mathbf{x}}$ and put it into Eqn. 3 to look at the effects of the coupling constants g and v . Imagine that at a given pressure $p > p_{c1} = 25$ bar, if tuning $g \neq 0$, but keeping v intact, then the normal solid becomes an asymptotically P-H symmetric normal solid (NS-PH) in Fig. 3. Inside the NL, the mass of at $\mathbf{k} = 0$ is $t = T - T_{XY}$ which sets up the temperature scale of the problem. Inside the NS-PH, it is easy to see that the mass of at $\mathbf{k} = 0$ is $t_{NS-PH} = t + v \frac{0}{G} \int_0^0 n(G) \frac{1}{2}$. If we take the temperature scale $t = T - T_{XY}$ as the reference scale, then $t_{NS-PH} = T + \eta(p)$ where $\eta(p) = v \frac{0}{G} \int_0^0 n(G) \frac{1}{2} - T_{XY} > 0$ is the $T = 0$ gap for the local superuid mode at $\mathbf{k} = 0$ in the NS-PH. Because as the pressure p increases, the repulsive interaction v also increases, so it is reasonable to assume that $\eta(p)$ is a monotonic increasing function of p . Because it is a first order transition across p_{c1} , just like the roton gap $\eta_r > 0$ remains finite just before the first order transition, $\eta(p)$ also remains finite just after the first order transition, namely, $\eta(p_{c1}^+) > 0$ (Fig. 3).

Taking this NS-PH as a reference state, we then grad-

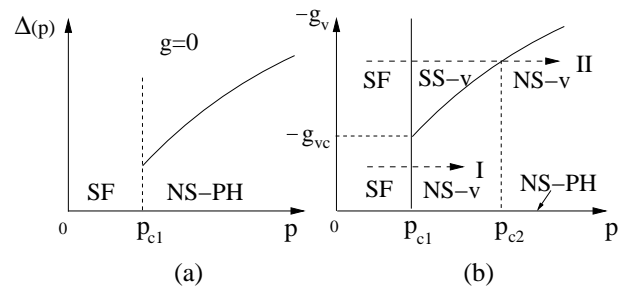


FIG. 3: (a) The gap $\Delta(p)$ of the local fluctuating superuid mode in the P-H symmetric commensurate normal solid (NS-PH) which exists only at $g = 0$. We assume it is a monotonic increasing function of the pressure p . (b) The zero temperature phase diagram of g_v versus the pressure p . The NS-PH only exists at $g_v = 0$. Any $g_v \neq 0$ will transfer the NS-PH into the NS-v. If the experimental is along the path I, then it is a direct 1st order SF to NS-v transition in Fig. 1, if it is along the path II, it is a 1st order SF to SS-v, then a 2nd order SS-v to NS-v transition in Fig. 2.

ually turn on g and see how the ground state evolves. In the presence of the periodic potential of $n(\mathbf{x})$ lattice, will form a Bloch wave, the interaction u in Eqn 2 will certainly favor extended Bloch wave over strongly localized Wannier state. In principle, a full energy band calculation incorporating the interaction u is necessary to get the energy bands of . Fortunately, qualitatively important physical picture of GL Eqs. 1, 2, 3 can be achieved without such a detailed energy band calculation. Neglecting the self interaction u which is not important in the extended Bloch states and taking $g \neq 0$ as a small parameter, A perturbative estimate on the eigenenergy

(0) at the origin $\mathbf{k} = 0$ up to the third order g^3 is:

$$(0) = t - g^2 P \frac{n^2(G)}{K G^2} + g^3 \frac{X^0 X^0}{K G_1^2 K G_2^2} \frac{n(G_1) n(G_2) n(G_1 - G_2)}{G_1 G_2} + \quad (18)$$

where the term linear in g vanishes, v stands for vacancies and interstitials respectively and $G = 2 = a$ with a 3.17 \AA the lattice constant of the solid ^4He , the $n(G_1) = e^{G^2 a^2/4}$ can be taken as a Gaussian where is the width of the Gaussian.

In reality, g may be large, so we may need to go beyond leading order. For vacancies, $g_v < 0$, without writing out the coefficients explicitly, the expansion is

$$\eta_v(0) = t - g^2 - g^3 - g^4 + \quad (19)$$

so the coefficient has the same sign. Assuming the series converges, for any $g_v < 0$, we can write $\eta_v(0) = t - f_v(g_v)$ where the $f_v(g_v) > 0$; $f_v(0) = 0$ is a monotonic increasing function of g_v and likely has no upper bound.

For interstitials, $g_i > 0$, without writing out the coef-

clients explicitly, the expansion is

$$_i(0) = t \quad \frac{g_i^2}{2} + g_i^3 \quad \frac{g_i^4}{4} +$$

so the coefficient has oscillating sign. Assuming the series converges, we can write $g_i(0) = t f_i(g_i)$ which holds for any g_i . Because of the oscillating nature of the expansion coefficients, it is hard to judge the nature of the function of $f_i(g_i)$ except we are sure $f_i(0) = 0$. The different expansion series of $f_v(g_v)$ and $f_i(g_i)$ indicate that quantum fluctuations may favor vacancies over interstitials. However, for simplicity, we assume $f_i(g_i)$ is also a monotonic increasing function of g_i , so we can discuss vacancies and interstitials induced supersolids on the same footing. In the following, we discuss SS-v and SS-i respectively.

A . Vacancies induced supersolid: SS-v

The mass of v was decreased to $t_v = T + \langle p \rangle$ $f_v(g_v) = T - T_{SS-v}$ where $T_{SS-v}(p) = f_v(g_v) - \langle p \rangle$ (Fig 2). Because $f_v(g_v)$ is a monotonic increasing function of g_v and $f_v(0) = 0$, defining a critical value $f_v(g_{vc}) = (p_{c1})$, then when $g_v > g_{vc}$, $f_v(g_v) < (p_{c1})$, the mode remains massive, namely $\langle v \rangle = 0$. The C-NS remains to be the ground state even at $T = 0$. It is important to stress that even the solid is a C-NS, it still does not have the P-H symmetry. For $g_v < 0$, the C-NS is a vacancy-like C-NS (named as NS-v) where the vacancy excitation energy v is lower than that of the interstitial i (Fig 1b).

If $g_v > g_{vc}$, then $T_{SS-v}(p_{c1}) = f_v(g_v) - \langle p \rangle$ is raised above the zero temperature, the SS-v state exists in the Fig 1b. $T_{SS-v}(p_{c1})$ is also proportional to the superfluid density measured in the experiments. The resulting solid is an incommensurate solid with vacancies even at $T = 0$ whose condensation leads to $\langle v \rangle \neq 0$. Of course, the number of vacancies n_v is quite small. The SS-v state has a lower energy than the NS-v state at sufficiently low temperature. As the pressure increases to p_{c2} , $T_{SS-v}(p_{c2}) = f_v(g_v) - \langle p \rangle = 0$ (Fig 2). Then $f_v(g_v) = \langle p \rangle$, so $T_{SS-v}(p) = \langle p \rangle$ which becomes an effective experimental measure of the attractive coupling g_v in Eqn 3. In the following, substituting the ansatz $\langle 1(x) \rangle = ae^{i\omega_1 x}$ and $\langle 2(x) \rangle = e^{i\omega_2 x} \sum_{m=1}^P e^{iQ_m x}$ where $Q_m = Q$ into Eqn 3, we study the effects of lattice on $\omega = \omega_1 + \omega_2$. From Eqn 3, we can see $n(x)$ acts as a periodic potential on

. In order to get the lowest energy ground state, we must consider the following 4 conditions: (1) because any complex (up to a global phase) will lead to local supercurrents which is costly, so we can take ω to be real, so Q_m have to be paired as anti-nodal points. P has to be even (2) as shown from the Feynman relation Eqn 10, $Q_m; m = 1; \dots; P$ are simply P shortest reciprocal lattice vectors, then translational symmetry of the lattice dictates that $\mathbf{K} = 0 = \mathbf{K} = Q_m$, ω_1 and ω_2

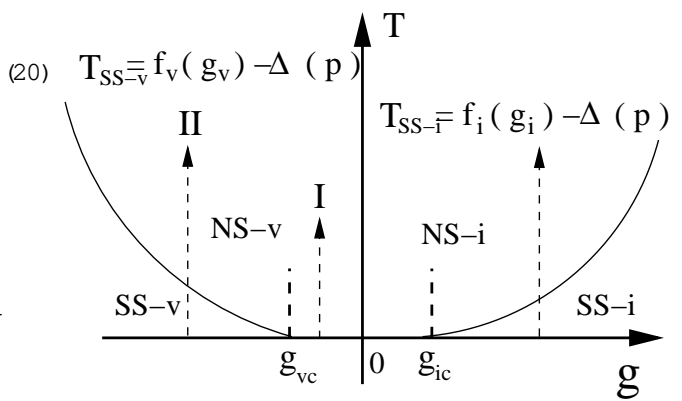


FIG . 4: The phase diagram of T versus g at a given pressure $p_{c1} < p < p_{c2}$. The finite temperature transitions denoted by the dashed line II at a given $g_v > g_{vc}$ (or $g_i > g_{ic}$) is in the 3D XY universality class described by Eqn 24. However, if $g_v < g_{vc}$, then the ground state at $T = 0$ is a vacancy-like C-NS (named as NS-v). Similar thing can be defined for an interstitial-like C-NS (named as NS-i) when $g_i < g_{ic}$.

have to condense at the same time (3) The point group symmetry of the lattice dictates $\omega_m = \omega$ and is real

(4) for the vacancies case, the interaction is attractive $g_v < 0$, from Eqn 3, the SDW wave simply sits on top of the lattice, so the Superfluid Density wave $\omega = \omega$ simple sits on top of the lattice as much as possible. This is reasonable, because vacancies are hopping on near the lattice sites, so the Bose condensation of vacancies also happen near the lattice sites. From Eqn 3, the attractive interaction also favors $\omega = \omega$ where $R=2$ stands for any interstitial sites which are in the middle of lattice points. It turns out that the 4 conditions can fix the relative phase and magnitude of ω_1 and ω_2 to be $\omega_2 = \omega_1$; $\omega = a = P$, namely:

$$\omega_{SS-v} = \omega_0 (1 + \frac{2}{P} \sum_{m=1}^{R=2} \cos Q_m \omega x) \quad (21)$$

where $\omega_0 = ae^{i\omega x}$ depends on the temperature and pressure. Note that in contrast to a uniform superfluid, the magnitude of ω is changing in space. This field satisfies the Bloch theorem with the crystal momentum $\mathbf{K} = 0$ and the Fourier components are $(\mathbf{K} = 0) = a$; $(\mathbf{K} = Q_m) = a = P$. They have the same sign and decay in magnitude. In principle, higher Fourier components may also exist, but they decay very rapidly, so can be neglected without affecting the physics qualitatively.

B . Interstitial induced supersolid: SS-i

The discussion is quite similar to the vacancy case except that (1) if $g_i < g_{ic}$, the C-NS is an interstitial-like C-NS (named as NS-i) where the interstitial excitation energy i is lower than that of the vacancy v (2) if

$g_i > g_{ic}$, the resulting solid is an in-com m ensurate solid with interstitials even at $T = 0$ whose condensation leads to $\langle \hat{n}_i \rangle \neq 0$, the SS-i state exists in the Fig 2. The arguments to determine the lattice structure of the SS-i goes the same as those in the vacancies case except the condition (4), for the SS-v, the interaction is attractive $g_v < 0$, the SDW-v simply sits on top of the n lattice. However, for the interstitials case, the interaction is repulsive $g_i > 0$ favors $\langle \hat{n}_i \rangle = 0$, so the Super uid Density wave $= j \hat{j}$ can avoid the n lattice as much as possible. This is reasonable, due to the competing of the two orders, the super uid component emerges from the places where the normal solid component is suppressed. It turns out that the the 4 conditions can x the relative phase and magnitude of α_1 and α_2 to be $\alpha_2 = \alpha_1 + \alpha_3$; $\alpha_3 = a = P$, namely:

$$s_{ss,i} = \alpha_0 (1 - \sum_{m=1}^{2^P} \cos Q_m \cdot \mathbf{x}) \quad (22)$$

where $\alpha_0 = ae^i$ depends on the temperature and pressure. Note that the crucial sign difference from the vacancies case which make an important difference from the X-ray scattering from SS-v and SS-i to be discussed in the next section. Again in contrast to a uniform super uid, the magnitude of α is changing in space. This field satisfies the Bloch theorem with the crystal momentum $\mathbf{K} = 0$ and the Fourier components are

$(\mathbf{K} = 0) = a$; $(\mathbf{K} = Q_m) = a = P$. They oscillate in sign and decay in magnitude. In principle, higher Fourier components may also exist, but they decay very rapidly, so can be neglected without affecting the physics qualitatively.

In the following, we will discuss different lattice structures of n when $P = 2, 4, 6, 8, 12$ respectively. Obviously, the Super uid Density wave $= j \hat{j}$ has the same Bravais lattice structure as the the n lattice. However, as shown in the following, even n is a Bravais lattice, the SDW may be the same Bravais lattice plus a few basis.

(a) $P=2$: $Q_1 = Q_2 = Q$ are a pair of anti-nodal points. They are the two shortest reciprocal lattice vectors generating a 1 dimensional lattice embedded in a 3 dimensional system. The field is $(\mathbf{x}) = a(1 - \cos Q \cdot \mathbf{x})$. There is a super uid density wave formation transition inside the normal solid which is a 2nd order transition in the universality class of 3D XY model (Fig 2). The local SDW operator $\hat{j}_s^1 = j(\mathbf{x})\hat{j} = a^2(1 - \cos Q \cdot \mathbf{x})$. It breaks translational invariance only along 1-dimension which is similar to Smectic-A or Smectic-C phase in the liquid crystal²⁸. The maxima of the SDW $_{max} = 2a$ appear exactly in the middle of lattice points at $\mathbf{a} = \frac{1}{2}\mathbf{a}_1$. So the SDW forms the dual lattice of the 1d lattice which is also a 1d lattice.

(b) $P=4$: $Q_3 = Q_1; Q_4 = Q_2; Q_1 \cdot Q_2 = 0$, $Q_i; i=1, 2, 3, 4$ form the 4 corners of a square. They are the four shortest reciprocal lattice vectors generating a 2 dimensional square lattice embedded in a 3 dimensional

system. The field is $(\mathbf{x}) = a[1 - \frac{1}{2}(\cos Q_1 \cdot \mathbf{x} + \cos Q_2 \cdot \mathbf{x})]$, The local SDW operator $\hat{j}_s^1 = j(\mathbf{x})\hat{j}$. The maxima of the SDW $_{max} = 2a$ appear exactly in the middle of lattice points at $\mathbf{a} = \frac{1}{2}(\mathbf{a}_1 + \mathbf{a}_2)$. So the SDW forms the dual lattice of the square lattice which is also a square lattice.

(c) $P=6$: there are two cases need to be discussed separately. (c1) $Q_i; i=1, 2, 3, 4, 5, 6$ form the 6 corners of a hexagon. They consist of the 6 shortest reciprocal lattice vectors generating a 2 dimensional triangular lattice embedded in a 3 dimensional system. The field is

$(\mathbf{x}) = a[1 - \frac{1}{3}(\cos Q_1 \cdot \mathbf{x} + \cos Q_2 \cdot \mathbf{x} + \cos Q_3 \cdot \mathbf{x})]$. The maxima of the SDW $_{max} = 3=2a$ appear in the middle of lattice points at $\mathbf{a} = \frac{1}{3}(\mathbf{a}_1 + \mathbf{a}_2)$. They form the dual lattice of the triangular lattice which is a honeycomb lattice. The honeycomb lattice is not a Bravais lattice which has two triangular sublattices A and B, it can be considered as one triangular lattice A plus a basis. This can be understood intuitively: there are two equivalent ways to shift the n lattice, one way to get the sublattice A, the other to get the sublattice B. Putting A and B together forms the SDW which takes the honeycomb lattice (c2) $Q_i; i=1, 2, 3, 4, 5, 6$ are the 6 shortest reciprocal lattice vectors generating a cubic lattice. The maxima of the SDW $_{max} = 2a$ appear exactly in the middle of lattice points at the 8 points $\mathbf{a} = \frac{1}{2}(\mathbf{a}_1 \pm \mathbf{a}_2 \pm \mathbf{a}_3)$. So the SDW forms the dual lattice of the cubic lattice which is also a cubic lattice.

(d) $P = 8$: $Q_i; i=1, \dots, 8$ form the 8 shortest reciprocal lattice vectors generating a bcc reciprocal lattice which corresponds to a fcc direct lattice. The field is

$(\mathbf{x}) = a[1 - \frac{1}{4}(\cos Q_1 \cdot \mathbf{x} + \cos Q_2 \cdot \mathbf{x} + \cos Q_3 \cdot \mathbf{x} + \cos Q_4 \cdot \mathbf{x})]$. The maxima of the SDW $_{max} = 2a$ appear in all the edge centers such as $(1=2; 0; 0)$ etc. and the centers of any cube such as $(1=2; 1=2; 1=2)$ etc. It is easy to see these points can be achieved by simply shifting the n lattice by $(1=2; 1=2; 1=2)$, so the SDW also forms a fcc direct lattice.

(e) $P = 12$: $Q_i; i=1, \dots, 12$ form the 12 shortest reciprocal lattice vectors generating a fcc reciprocal lattice which corresponds to a bcc direct lattice. The field is

$(\mathbf{x}) = a[1 - \frac{1}{6}(\cos Q_1 \cdot \mathbf{x} + \cos Q_2 \cdot \mathbf{x} + \cos Q_3 \cdot \mathbf{x} + \cos Q_4 \cdot \mathbf{x} + \cos Q_5 \cdot \mathbf{x} + \cos Q_6 \cdot \mathbf{x})]$. The maxima of the SDW $_{max} = 4=3a$ appear along any square surrounding the center of the cube such as $(1=2; 0; 0)$ or $(1=2; 0; 0)$ etc. In fact, one can achieve the SDW lattice by shifting the the center of bcc to the 3 face centers, so all these points are on the edge centers and face centers which are only discrete points on the square surrounding the center of the cube. We expect the continuous whole square is due to the artifact of the approximation $\langle \hat{n}_i \rangle = 0$ imposed. So the SDW 4He in Vycor glass takes a bcc lattice.

Unfortunately, a spherical $k = Q$ surface can not lead to lattices with different lengths of primitive reciprocal lattice vectors such as a hcp lattice. This is similar to the classical liquid-solid transition described by Eqn 1 where a single maximum peak in the static structure factor can not lead to a hcp lattice²⁸. Another difficulty with the

hcp lattice is that the hcp lattice is not a Bravais lattice, it consists of two inter-penetrating simple hexagonal lattices shifted by $\mathbf{a} = \frac{1}{3}\mathbf{a}_1 + \frac{1}{3}\mathbf{a}_2 + \frac{1}{2}\mathbf{a}_3$. Here we can simply take the experimental fact that \mathbf{n} forms a hcp lattice without knowing how to produce such a lattice from a GL theory Eqn 1. Despite the technical difficulty, because for an ideal hcp lattice $c/a = \sqrt{8/3}$, an hcp lattice has 12 nearest neighbors, so its local environment may resemble that of an fcc lattice. We expect the physics (except the anisotropy of NCR1 in the hcp lattice to be discussed in the next two sections) is qualitatively the same as that in fcc direct lattice. From the insights achieved from the other lattices, one can achieve the SDW lattice by shifting the hcp lattice of \mathbf{n} by $\mathbf{a} = \frac{2}{3}(\mathbf{a}_1 + \mathbf{a}_2) + \frac{1}{4}\mathbf{a}_3$.

C. Discussions on both SS-v and SS-i

In fact, for both SS-v and SS-i, we can write \mathbf{n} and \mathbf{P} in a more symmetric way: $\mathbf{n}(\mathbf{x}) = \mathbf{n}_0 + \mathbf{P}_0 \mathbf{n}_G e^{iG \cdot \mathbf{x}}$; $\mathbf{P}(\mathbf{x}) = \mathbf{P}_0 \mathbf{n}_G e^{iG \cdot \mathbf{x}}$. It is easy to see that in the SS, the translational symmetry $\mathbf{x} + \mathbf{a}; \mathbf{n}_G + \mathbf{n}_G e^{iG \cdot \mathbf{a}}$; $\mathbf{P}_0 + \mathbf{n}_G e^{iG \cdot \mathbf{a}}$ is broken down to $\mathbf{a} = \mathbf{R}; \mathbf{n}_G + \mathbf{n}_G e^{iG \cdot \mathbf{R}} = \mathbf{n}_G; \mathbf{P}_0 + \mathbf{n}_G e^{iG \cdot \mathbf{R}} = \mathbf{n}_G$. In the Fig 2, in the NL side, as the temperature is lowered, the symmetry breaking happens in $\mathbf{1}$ at $\mathbf{k} = 0$, the NL gets into the SF. However, as shown in this section, in the NS side, the symmetry breaking happens in both the $\mathbf{1}$ at $\mathbf{k} = 0$ and $\mathbf{2}$ sector at \mathbf{P} discrete points in a spherical surface $\mathbf{k} = \mathbf{Q}$ simultaneously, the NS gets to the SS state at a much lower critical temperature T_{SS} . The results achieved from the NS side in this section indeed complement Fig 2 achieved from the roton condensation picture in the SF phase in the last section.

VII. EXCITATIONS IN THE SUPERSOLID

So far, we only look at the mean field solutions corresponding to vacancies and interstitials. Here we discuss excitations above the mean field solutions. It turns out that the excitations in both cases are the same, so we discuss both cases at same time. In the SS-v and SS-i, the wavefunctions can be written as

$$\psi_{ss} = \psi_0 (1 - \sum_{m=1}^2 \sum_{k=1}^{K=2} \cos Q_m \cdot \mathbf{x}); \quad \psi_0 = j_0 \mathbf{j}^1 \quad (23)$$

where ψ sign corresponds to SS-v and SS-i respectively. Obviously, there are also topological defects in the phase winding of which are vortices. At $T = T_{SS}$, the vortices can only appear in tightly bound pairs. However, as $T > T_{SS}$, the vortices start to become liberated, this process renders the total NCR1 to vanish above $T > T_{SS}$. In addition to the superuid mode in SS states, there are also lattice phonon modes in both \mathbf{n} sector and $\mathbf{2}$ sector. However, it is easy to see that the coupling Eqn 3

is invariant under $\mathbf{x} + \mathbf{a}; \mathbf{n}(\mathbf{G}) + \mathbf{n}(\mathbf{G}) e^{iG \cdot \mathbf{a}}$; $\mathbf{G} + \mathbf{a}$

$\mathbf{G} e^{iG \cdot \mathbf{a}}$, so the lattice phonon modes in are locked to those in the conventional lattice³⁶. This is expected because there is only one kind of translational symmetry breaking, therefore only one kind of lattice phonons. The coupling between the mode and the umode was worked out in²⁹. If ignoring the coupling between the superuid mode and the phonon mode, then the action to describe the NS to SS transition in a static lattice is:

$$f_0 = K_{NS} j_0^2 + t_{NS} j_0^2 + u_{NS} j_0^4 + \dots \quad (24)$$

where $t_{NS} = T_{SS}$ and $T_{SS}(\mathbf{p}) = f_v(g_v) = (p_{c2})$ and $T_{SSi}(\mathbf{p}) = f_i(g_i) = (p_{c2})$. Obviously, it is still a 3d XY transition. It was shown in¹⁵ that the coupling to the phonon mode will not change the universality class at finite temperature. As the pressure increased to p_{c2} , T_{SSv} or T_{SSi} are suppressed to zero, the system becomes a C-NS where $\langle \dots \rangle = 0$. It is important to stress that even at $p > p_{c2}$, the solid is a C-NS, it still does not have the PH symmetry because $g \neq 0$. For $g_v < 0$, the C-NS is vacancy like (NS-v) where the vacancy excitation energy is lower than that of the interstitial. For $g_i > 0$, the C-NS is interstitial like (NS-i) where the interstitial excitation energy is lower than that of the vacancy. The zero temperature transition from the SS-v (SS-i) to the NS-v (NS-i) driven by the pressure near $p = p_2$ will be studied in²⁹. A low energy effective action involving the superuid phonon, the lattice phonons and their couplings will also be studied in²⁹.

In the SF phase, a single vortex costs a lot of energy $E_v^{SF} = \frac{s_F h^2}{4 m^2} \ln \frac{R}{a}$ where m is the mass of He atom, R is the system size and s_F is the core size of the vortex. This energy determines the critical velocity in SF $v_c^{SF} > 30 \text{ cm/s}$. Because the long distance behavior of SS is more or less the same as SF, we can estimate its single vortex energy $E_v^{SS} = \frac{s_{SS} h^2}{4 m^2} \ln \frac{R}{a}$ where s_{SS} is the global superuid density inside the SS. We expect the core size of a supersolid vortex $s_{SS} = 1 = 1 = k_F a / s_F$. So inside the SS vortex core, we should also see the lattice structure of n^{39} . This is similar to the phenomenon that DW ordered states were detected in the vortex core of high temperature superconductors^{37,38}. In fact, because

\mathbf{x} stands for vacancies or interstitials, we expect that s_{SS} should be of the order of the average spacing between the interstitials or vacancies in the SS. It is interesting to see if neutron or light scattering experiments can test this prediction. Compared to E_v^{SF} , there are two reductions, one is the superuid density, another is the increase of the vortex core size s_{SS} / s_F . These two factors contribute to the very low critical velocity $v_c^{SS} < 30 \text{ m/s}$. Of course, the reduction from the increase of the vortex core is negligible because of the logarithmic dependence.

V III. X-RAY SCATTERING FROM THE SS

Let's look at the prediction of our theory on X-ray scattering from the SS. For a lattice with $j = 1$; basis located at \mathbf{d}_j , the geometrical structure factor at the reciprocal lattice vector \mathbf{K} is $S(\mathbf{K}) = \sum_{j=1}^n f_j(\mathbf{K}) e^{i\mathbf{K} \cdot \mathbf{d}_j}$ where f_j is the atomic structure factor of the basis at \mathbf{d}_j . The X-ray scattering amplitude $I(\mathbf{K}) = \int \mathbf{K} \mathbf{f}(\mathbf{K})^2$. Again, we discuss SS-v and SS-i respectively.

A. X-ray scattering from the SS-v

In this case, because the superuid density wave simply sits on the n lattice, so the X-ray scattering is very similar to that from NS at mean field level. However, as shown in C, quantum and thermal fluctuations will still make the X-ray scattering from the SS-v different from that from the NS.

B. X-ray scattering from the SS-i

In this case, as shown in section V I, the superuid density wave is shifted from n lattice, so the X-ray scattering is different from that from NS even at mean field level. For simplicity, we first take the sc lattice to explain the main points, then list the X-ray scattering from all the other lattices classified in section V I.

(a) Simple Cubic lattice. For the SS in the sc lattice, as shown in (2) of the last section, the local superuid density attains its maximum at the dual lattice points of the sc lattice. Then $\mathbf{d}_1 = 0; \mathbf{l}_1 = \frac{a}{2}(\mathbf{i} + \mathbf{j} + \mathbf{k}); \mathbf{K} = \frac{2}{a}(n_1\mathbf{i} + n_2\mathbf{j} + n_3\mathbf{k})$, then taking the ratio of the geometrical structure factor of SS over that of the NS $S_{SS}(\mathbf{K}) = S_{NS} = 1 + f(1)^{n_1+n_2+n_3}$ where $f = \frac{m_{\text{ax}}}{s} \frac{a^2}{2}$. It is 1 + f for even \mathbf{K} and 1 - f for odd \mathbf{K} .

(b) Triangular lattice. $\mathbf{d}_1 = 0; \mathbf{l}_1 = \frac{1}{3}(\mathbf{a}_1 + \mathbf{a}_2); \mathbf{l}_2 = \frac{2}{3}(\mathbf{a}_1 + \mathbf{a}_2); \mathbf{K} = n_1\mathbf{b}_1 + n_2\mathbf{b}_2$, then taking the ratio of the geometrical structure factor of SS over that of the NS $S_{SS}(\mathbf{K}) = S_{NS} = 1 + 2f \cos \frac{2}{3}(n_1 + n_2)$. This result could be relevant to possible 2d excitonic superuid in electron-hole bilayer system to be briefly mentioned in section X.

(c) hcp lattice. hcp lattice is not a Bravais lattice. In NS, $\mathbf{d}_1 = 0; \mathbf{d}_2 = \frac{1}{3}(\mathbf{a}_1 + \mathbf{a}_2) + \mathbf{a}_3 = 2; \mathbf{K} = n_1\mathbf{b}_1 + n_2\mathbf{b}_2 + n_3\mathbf{b}_3$, then $S_{NS}(\mathbf{K}) = 1 + e^{i2(\frac{n_1+n_2}{3} + \frac{n_3}{2})}$. In the SS, there are 2 more additional basis at $\mathbf{l}_1 = \frac{2}{3}(\mathbf{a}_1 + \mathbf{a}_2) + \mathbf{a}_3 = 4; \mathbf{l}_2 = 3\mathbf{a}_3 = 4$, then $S_{SS}(\mathbf{K}) = S_{NS}(\mathbf{K}) + fe^{i2(\frac{2(n_1+n_2)}{3} + \frac{n_3}{4})} + fe^{i\frac{3}{2}n_3} = S_{NS}(\mathbf{K}) + fe^{i\frac{1}{2}n_3} S_{NS}(\mathbf{K})$.

(d) bcc lattice. We think bcc lattice as a sc lattice plus a basis, $\mathbf{d}_1 = 0; \mathbf{d}_2 = \frac{a}{2}(\mathbf{i} + \mathbf{j} + \mathbf{k}); \mathbf{K} = \frac{2}{a}(n_1\mathbf{i} + n_2\mathbf{j} + n_3\mathbf{k})$, Then $S_{NS}(\mathbf{K}) = 1 + (-1)^{n_1+n_2+n_3}$ which is 2 for even \mathbf{K} and 0 for odd \mathbf{K} . In the SS, there are 3 more additional basis at $\mathbf{l}_1 = \frac{a}{2}(\mathbf{i} + \mathbf{j}); \mathbf{l}_2 = \frac{a}{2}(\mathbf{i} + \mathbf{k}); \mathbf{l}_3 = \frac{a}{2}(\mathbf{j} + \mathbf{k})$,

, then $S_{SS}(\mathbf{K}) = S_{NS}(\mathbf{K}) + f[(-1)^{n_1+n_2} + (-1)^{n_1+n_3} + (-1)^{n_2+n_3}]$.

(e) fcc lattice. We think fcc lattice as a sc lattice plus 4 basis located at $\mathbf{d}_1 = 0; \mathbf{d}_2 = \frac{a}{2}(\mathbf{i} + \mathbf{j}); \mathbf{d}_3 = \frac{a}{2}(\mathbf{i} + \mathbf{k}); \mathbf{d}_4 = \frac{a}{2}(\mathbf{j} + \mathbf{k}); \mathbf{K} = \frac{2}{a}(n_1\mathbf{i} + n_2\mathbf{j} + n_3\mathbf{k})$, then $S_{NS}(\mathbf{K}) = 1 + [(-1)^{n_1+n_2} + (-1)^{n_1+n_3} + (-1)^{n_2+n_3}]$. In the SS, there is one more additional basis located at $\mathbf{l}_1 = \frac{a}{2}(\mathbf{i} + \mathbf{j} + \mathbf{k})$, then $S_{SS}(\mathbf{K}) = S_{NS}(\mathbf{K}) + f(-1)^{n_1+n_2+n_3}$. It is easy to see that in bcc and fcc lattices, we need simply exchange d vectors for the NS and the l vectors for SDW.

We conclude that the elastic X-ray scattering intensity from the SS-i has an additional modulation over that of the NS. The modulation amplitude is proportional to the maximum of the superuid density $\frac{m_{\text{ax}}}{s} \frac{a^2}{2}$ which is the same as the NCR observed in the PSU's torsional oscillator experiments.

C. Effects of Debye-Waller factors on SS-v and SS-i

Due to large zero-point motion in solid ${}^4\text{He}$, any X-ray scattering amplitude $I(\mathbf{K})$ will be diminished by a Debye-Waller factor. As shown in the last section, because the lattice phonon modes \mathbf{u} in are locked to those of n, so there is a common Debye-Waller factor $e^{-\frac{1}{3}K^2 \langle u^2 \rangle}$ coming from the large zero point motions in NS and SS. If ignoring the coupling between the superuid mode and the phonon mode, then by taking the ratio $I_{SS} = I_{NS}$, we expect this Debye-Waller factor drops out. However, the coupling may still make the Debye-Waller factors in SS-v and SS-i different than that in NS. How the Debye-Waller factor affects the X-ray scattering from the SS-v and SS-i will be discussed in²⁹.

Unfortunately, so far, the X-ray scattering data is limited to high temperature $T > 0.8\text{K} > T_{\text{SS}}$ ³⁵. X-ray scattering experiments on lower temperature $T < T_{\text{SS}}$ are being performed to test these predictions¹².

IX. THE NCRYO OF SF AND SS STATES AT $T = 0$ AND $T > 0$.

In order to calculate the superuid density s explicitly, we need to look at how the system's free energy responds to a fictitious gauge potential \mathbf{A} . We find that when $c_s(T = 0) = = d^d x j(\mathbf{x}; \mathbf{A}) = d^d x (j_1(\mathbf{x}; \mathbf{A}) + j_2(\mathbf{x}; \mathbf{A}))$ where the crossing term s between j_1 and j_2 drop out due to the momenta conservation. Note that although j_2 does not contribute to the condensate, it does contribute to the superuid density. This is consistent with the fact that although 90% ${}^4\text{He}$ are out of the condensate, they all contribute to the superuid density.

In the SF state, at low T, the quantum fluctuations induced by the pressure are important. Let's first look

at the quantum phase fluctuations. The phase fluctuation action is given by $L_p = \frac{1}{2g} \int_{\mathbb{R}^d} \frac{d^d k}{(2\pi)^d} \left(\frac{1}{n} + k^2 \right) j(\mathbf{k}; t) j(\mathbf{k}; 0)$ where $g = \frac{1}{s}$ controls the strength of quantum phase fluctuations and the super uid phonon velocity has been set equal to 1 for simplicity. It is easy to see that at $T = 0$, $\langle j^2(\mathbf{x}; t) \rangle_{T=0}$ is infra-red (IR) finite, so the quantum phase fluctuations alone will not lead to any instability. However, it will lead to super uid density depletion even before reaching the phase boundary of SF to SS transition in Fig.1 and Fig.2, although the depletion may be quite small. This fact explains why $T_{SF}(p)$ bends to the left slightly as the pressure p increases. At finite T , the thermal fluctuations $\langle j^2(\mathbf{x}; t) \rangle_T < \langle j^2(\mathbf{x}; t) \rangle_{T=0}$ T^{d-1} lead to $s(T) = s(T=0) \text{c}^{d-2}$ at $d=3$. It is well known the super uid density (T) $(T=0)$ at, while the Bose condensation density $n_b(T) = n_b(T=0) \text{b}^{d-2}$. So strictly speaking, n sector can only describe the bose condensation density. This is expected, because the n sector in the SF phase also contributes to the super uid density, but not to the BEC.

Then let's look at the roton fluctuations whose action is given by Eqn.8. Setting $\omega_2 = \omega_1^2$, at $T = 0$, the quantum roton fluctuations $\langle j_2^2(\mathbf{x}; t) \rangle_{T=0}$ $\log -$ is IR logarithmic divergent as $\omega_1 \rightarrow 0$ which signifies the instability to the lattice formation. Due to this IR divergence, the 1st order SF to SS transition may happen well before becomes zero, namely, at $\omega_1 = \omega_c > 0$. This is consistent with the picture described in sec. IV. At finite T , the thermal roton fluctuations $\langle j_2^2(\mathbf{x}; t) \rangle_T < \langle j_2^2(\mathbf{x}; t) \rangle_{T=0}$ $(\log -)e^{-\frac{T}{\omega_1}}$ when $T \rightarrow 0$.

In the SS-v and SS-i states, the $n(\mathbf{x})$ forms a lattice, at the same time, the unstable roton part is replaced by a stable SDW formation commensurate with the underlying n lattice. Obviously, the $n(\mathbf{x})$ normal lattice takes away the vast majority of density from the super uid density even at $T = 0$. The preliminary calculations in²⁹ showed that super uid density from the n_1 sector is isotropic $\langle j_1^2(\mathbf{x}) \rangle = K \delta^d$, while the super uid density from n_2 sector turns out to be anisotropic in hcp lattice $\langle j_2^2(\mathbf{x}) \rangle = \sum_{m=1}^P \sum_{ij} j_m^2 Q_{m,ij} = Q^2$ where $m = a = P$ for SS-v or SS-i. Therefore, the total super uid density in SS phase is:

$$\langle j^2(\mathbf{x}) \rangle_{SS} = \langle j_1^2(\mathbf{x}) \rangle + \langle j_2^2(\mathbf{x}) \rangle = K \delta^d + \frac{1}{P^2} \sum_{m=1}^P Q_{m,1} Q_{m,1} = Q^2 \quad (25)$$

Taking $P = 6$, the anisotropy is quite small. Solid ^4He in a bulk takes a hcp lattice with $c/a = 1.63$ which is quite close to the idea value $c/a = \sqrt{8/3}$. The three primitive reciprocal lattice vectors are $\mathbf{G}_1 = \mathbf{G}_2 = \frac{4\pi}{3a} \hat{\mathbf{a}}$; $\mathbf{G}_3 = \frac{2\pi}{c} \hat{\mathbf{c}}$. We can estimate the anisotropy of the NCR1 in the hcp lattice. If the rotation axis is along the $\hat{\mathbf{c}}$ axis, the NCR1 is $\langle j^2(\mathbf{x}) \rangle = K \delta^d + v_r \sum_{m=1}^6 j_m^2 Q_{m,1} Q_{m,1} = Q^2$. If the rotation axis is along the $\hat{\mathbf{a}}$ (or $\hat{\mathbf{b}}$) axis, the NCR1 is $\langle j^2(\mathbf{x}) \rangle = K \delta^d + v_r \sum_{m=1}^6 j_m^2 Q_{m,3} Q_{m,3} = Q^2$. The anisotropy mainly comes from the n_2 sector. Setting

$s = G_1 = G_3$, for the idea value $s = \frac{4\pi^2}{3} > 1$, so $\langle j^2(\mathbf{x}) \rangle_{SS} > \langle j^2(\mathbf{x}) \rangle_{NCR1}$. Namely, the NCR1 response is larger when one is rotating the sample around the $\hat{\mathbf{c}}$ axis than that when one is rotating the sample around the $\hat{\mathbf{a}}$ or $\hat{\mathbf{b}}$ axis. However, as the pressure is increased, s decreases, the anisotropy of the NCR1 also decreases. In the P SU experiments, the samples are poly-crystal, the relative orientation of the rotation axis to the $\hat{\mathbf{c}}$ axis is not known, so it's hard to test this prediction with poly-crystals.

X. COMPARISONS WITH SUPER-SOLID SONS LATTICES

Supersolids on lattice models were studied in⁴¹. The GL theory, especially the coupling between n sector and j sector in⁴¹ are different than those in Eqn 1, Eqn 2, Eqn 3 in bulk ^4He system constructed in this paper. In⁴¹, due to the lack of components in non-zero reciprocal lattice vectors \mathbf{G} , the first non-trivial coupling is the quartic term $\int_{\mathbb{R}^d} \frac{1}{\pi} \sum_{\mathbf{G}} v_{\mathbf{G}} j_{\mathbf{G}} j_{\mathbf{G}}^* j_{\mathbf{G}}^*$. Indeed, if we only consider the mode near $\mathbf{k} = 0$, then the v term in Eqn 3 reduces to this term. In Eqn 3, we also have the most important additional cubic term $\int_{\mathbb{R}^d} \frac{1}{\pi} \sum_{\mathbf{G}} v_{\mathbf{G}} j_{\mathbf{G}} j_{\mathbf{G}}^* j_{\mathbf{G}}^*$ in Eqn 3. This crucial difference make the two GL theories completely differently.

In⁴², we studied all the possible phases and phase transitions in an extended boson Hubbard model in bipartite lattices such as a honeycomb and square lattice near half filling. We show that there are two consecutive transitions at zero temperature driven by the chemical potential: in the Ising limit, a Commensurate-Charge Density Wave (CDW) at half filling to a narrow window of CDW supersolid, then to an Incommensurate-CDW; in the easy-plane limit, a Commensurate-Valence Bond Solid (VBS) at half filling to a narrow window of VBS supersolid, then to an Incommensurate-VBS. The first transition is second order in the same universality class as the Mott to insulator transition, therefore has the exact critical exponents $z = 2$; $\nu = 1/2$; $\beta = 0$ with logarithmic corrections, while the second one is first order. Liu and Fisher⁴¹ also studied the CDW to the CDW-SS transition and concluded that $z = 1$ in contrast to $z = 2$ achieved in⁴². We found that the phase diagram in the Ising limit is similar to the reentrant "super uid" in a narrow region of coverages in the second layer of ^4He adsorbed on graphite detected by Crowell and Reppy's torsional oscillator experiment in 1993⁴⁴. It is still not clear if the extended boson Hubbard model can describe the experimental situation well. But the results suggest that ^4He lattice supersolid may have been already observed in 1993 which was 11 years earlier than the P SU's experiments on bulk ^4He . Indeed, the data in the torsional oscillator experiment in⁴⁴ do not show the characteristic form for a 2d ^4He super uid in, instead it resembles that in⁷ characteristic of a supersolid in terms of the gradual onset temperature of the NCR1, the unusual temperature dependence of T_{SS} on the coverage.

Of course, both experiments may due to phase separations instead of the SS phase. very recently, the author studied various kinds of supersolids in frustrated lattices such as triangular and kagomé lattices⁴³.

It is known that a lattice system is different than a continuous system in many ways. So the reentrant lattice SS discussed in^{41,42,43} is different from the bulk ⁴He SS state discussed in this paper, although both kinds of supersolids share many interesting common properties. In both cases, the SF to SS transition is driven by the closing of the gap of the roton minimum. On the lattice, the manifold of the roton minimum consists of discrete points due to the lattice symmetry, so the transition could be 1st or second order. However, in ⁴He, as shown in sections III and IV, the manifold of the roton minimum is a continuous surface, so the transition must be 1st order. In the former, there is a periodic substrate or spacer potential which breaks translational symmetries at the very beginning. The filling factor is controlled by an external chemical potential. There are particle-hole symmetry for excitations at integer filling factors which ensure the number of particles is equal to that of vacancies and at half filling factors which ensure adding interstitials is equivalent to adding vacancies^{42,43}. While in the latter, the lattice results from a spontaneous translational symmetry breaking driven by the pressure as shown in the Fig 2, if there are vacancies or interstitials in the ground state has to be self-determined by ground state energy minimization. There is usually no particle-hole symmetry for excitations. Due to this absence of symmetry, the number of vacancies is usually not equal to that of interstitials. So the theory developed in this paper on bulk ⁴He is different from the lattice theory developed in^{41,42}. As shown in the appendix and in^{42,43}, one common fact of both supersolids is that both are due to vacancies or interstitials. Lattice supersolids can also be described by doping the adjacent CDW either by vacancies or interstitials, so are classified as two types SS_v and SS_i. In the hard-core limit, SS_v and SS_i are simply related by P-H transformation. However, as shown in section VI, in Helium-4 supersolid, there is no particle-hole symmetry relating $T_{SS\ v}$ to $T_{SS\ i}$ (Fig.3) ! So the coupling constant g in Helium-4 plays a similar role as the chemical potential in the lattice models, the gap (ρ) in the NS-PH which tunes the distance from the NS-PH to the SF plays a similar role as the gap in the CDW which tunes the distance from the CDW to the superuid. It was shown in⁴³, the lattice supersolids existing at commensurate 1/2 filling factors in frustrated lattices such as triangular lattice is just the coexistence of SS_v and SS_i. Combined with the results in⁴², we conclude that ⁴He supersolid can exist both in bulk and on substrate, while although ⁴He₂ supersolid may not exist in the bulk, but it may exist on wisely chosen substrates. Lattice supersolid could also be realized in optical lattices in ultra-cold atomic experiments^{6,47}. However, in both continuum and on lattices, SS states could be unstable against phase separations. For example, the vacancies

or interstitials in the in-commensurate solid can simply move to the boundary of the sample instead of boson condensation, namely, it will turn into a commensurate solid. This case is included in the C-NS case in the paper anyway. Due to its negative compressibility, the instability of lattice SS against phase separation was demonstrated in some lattice models in^{48,49}.

X I. DISCUSSIONS ON PSU'S AND OTHER EXPERIMENTS AND APPLICATIONS IN OTHER SYSTEMS

1. The effects of He3 impurities

Although the NS to SS transition is in the same universality class as the NL to SF one, it may have quite different α -critical behaviours due to the SDW structure in the SS state. We can estimates the critical regime of the NS to SS transition from the Ginsburg Criterion $t_G^{1/3} \ll C$ where C is the specific jump in the mean field theory. Because of the cubic dependence on α , large α leads to extremely narrow critical regime, the 3D XY critical behavior is essentially irrelevant, instead mean field Gaussian theory should apply. Assuming ³He impurities diffusion process is slow, we can use this fact to address two experimentally observable effects of the He3 impurities. As said in the introduction, the first one was already observed by the PSU experiments¹². The second one was just being observed¹². (1) slightly below T_{SS} , the vortex pairs are in the dilute vortex limit where the unbinding transition temperature T_{SS} is determined by the pinning due to impurities instead of by the logarithmic interactions between the vortices which is proportional to the superuid stiffness. So the He3 impurities effectively pin the vortices and raise the unbinding critical temperature T_{SS} . Taking the He3 impurity concentration $x = 0.3\text{ppm}$, the average distance d_{imp} between the He3 impurities is $d_{imp} = 45\text{\AA} = 120a$, the average distance between a vortex pair is $R_p > \sqrt{ss}a$, we expect $R_p \gg d_{imp}$, the vortex pair is indeed effectively pinned by the He3 impurities at such a tiny concentration. On the other hand, He3 impurities will certainly decrease the superuid density in both the ₁ and ₂ sector just like He3 impurities decreases superuid density in the ⁴He superuid. Note that in ⁴He superuid, slightly below T_{SF} , the vortex pairs are in the dense vortex limit where the unbinding transition temperature T_{SF} is determined by the logarithmic interactions between the vortices which is proportional to the superuid stiffness. So in ⁴He SF, He3 impurities hurt superuid density which, in turn, lead to the reduction in T_{SF} . In short, the He3 impurities play a dual role in the SS phase, on the one hand, they raise the unbinding critical temperature T_{SS} of the vortices, on the other hand, they decrease the superuid density in both ₁ and ₂ sector. Indeed, in the PSU's experiments, in an isotropically stressed sample, as the concentration of He3 impurities decreases, the T_{SS} drops considerably,

but the NCR I rises. In contrast, in both 3d super uid ^4He and 2d super uid ^4He in s, He3 impurities hurt both the super uid sti ness and T_c . So the role played by He3 impurities in the PSU experiments is similar to the disorder played in fractional quantum Hall effects: the disorder is needed to even have a fractional quantized Hall plateau, but the quantum Hall liquid ground state is completely due to the strong Coulomb interaction among electrons and exists even in the absence of disorder. However, too much disorder will also destroy the fractionally quantized Hall plateau just like too much He3 impurities will also destroy the super uid density. (2) In principle, in clean system, the specific heat measurement should show the peak as the NL to SF transition does. Because the 3d XY specific heat exponent $= 0.012 < 0$, from the Harris criterion, we conclude that weak disorder will not change the universality class of the 3d XY model describing the SS to the NS transition, so will not destroy the peak. However, due to very narrow critical regime, it will be very difficult to observe the peak. So the 3D XY critical behavior of the NS-SS transition is essentially irrelevant in the PSU experiments, instead mean field Gaussian theory should apply where there should be a specific heat jump at $T = T_{SS}$. The mean field jump may be smeared by the presence of He3 impurities. Indeed, recent very refined specific heat measurements indeed found a broadened specific heat peak around 100m K when $x = 0.3$ 3 ppm¹². We conclude that the broadened specific heat peak around 100m K in the presence of He3 impurities is closely related to the opposite trend of the dependence of T_{SS} and the super uid density on the concentration of He3 impurities.

2. Non-equilibrium behavior in the torsional oscillator experiments

In principle, the super uid density should scale as $s(T_c - T)$ in the critical regime where 0.67 for the 3D XY model. Again, due to the very narrow critical regime, this scaling will not be seen. The experiment⁸ found that the NCR I slides towards the normal solid side with a very long tail. As argued in¹⁶, this behavior may be attributed to the non-equilibrium effects of the torsional oscillator experiments.

3. Other torsional oscillator, mass flow and acoustic wave experiments

Recently, a Cornell group lead by Reppy found that the NCR I signal detected by the PSU group can be eliminated through a crystal annealing process¹⁸. There are two possible explanations for this observation (1) This corresponds to $j_{v,j} > j_{v,c,j}$ where the Fig 2 holds. There could be vacancies in the thermodynamic stable ground state whose condensation leads to the SS-v in the Fig 2. The annealing process simply push the He3 impurities to the boundary, so reduces the supersolid transition temperature T_{SS} as discussed in this section. (2) This corresponds to $j_{v,j} < j_{v,c,j}$ where the Fig 1 holds. A state with vacancies is just a metastable state, then the supersolid state is just a metastable state. Annealing not only gets rid of the He3 impurities, but also vacancies,

so reduce or eliminate the metastable SS-v state. Even so, a SS-v metastable state maybe interesting and deserves the investigations done in this paper. Note that the Cornell's experiment itself may be controversial. The PSU group did the same annealing process which, in fact, last much longer than Cornell's group did, so should result even better crystal with even better quality, but the supersolid signal (NCR I effect) stays more or less the same¹². One of the main points of the manuscript is that the X-ray scattering experiment on SS-v, if can be performed at low enough temperature, can be very helpful to resolve the debate.

Beamish's group¹⁹ found that there is no detectable mass flow driven by pressure difference in solid Helium in Vycor at temperature as low as 48 m K and pressure 60 bar. It is possible that the response of the SDW in the SS to the pressure difference may be quite different than a uniform SF. It is important to work out this response. In another word, it is important to resolve the puzzle that why the SDW behaves like a super uid in the torsional oscillator experiment, but does not response sensitively to a pressure difference.

By acoustic attenuation and heat wave experiments⁴⁰, Goodkind discovered that the solid ^4He displays a phase transition below 200 m K only if it is strained or in the presence of He3 impurities also in the concentration range of ppm. This observation is consistent with the PSU's torsional oscillator experiments. The mechanism proposed above may also lead to a natural explanation of Goodkind's observation.

4. Absence of supersolid in solid hydrogen

The solid (para)-hydrogen H_2 also takes the hcp lattice. As explained in the introduction, so far, no NCR I was discovered in H_2 solid. Although H_2 are even lighter than ^4He , it has deeper attractive potential, so smaller de Boer quantum number. Bulk H_2 solidizes at $T < T_c = 14\text{K}$ even at zero pressure, this fact preempts the possible observation of the speculated SF state. At $T = 0$, due to the absence of the adjacent SF state, the quantum fluctuations are not strong enough to produce vacancies or interstitials in the H_2 solid, so the solid is a commensurate solid. Therefore, no SS is possible. As shown in section VI, approaching from the SF side, the vacancies or interstitials originate from the condensation of rotons, so in a continuous system, a SS state can not exist without the existence of an adjacent SF state in the first place. We conclude there is no supersolid in H_2 . One potential avenue to prevent p H_2 from being solidified to low enough temperature such that the super uid behavior can be observed is by depositing H_2 on external substrates which can disrupt the deep H_2 potential. It was suggested in⁴² that a judicious choice of substrate may be able to lead to an occurrence of hydrogen lattice supersolid.

5. Possible excitonic supersolids in fermionic systems

Although 2d bilayer quantum Hall system (BLQH) is a fermionic system, it was argued there exists excitonic super uid (ESF) state in the pseudo-spin channel⁵¹. In

real space, one exciton is an electron in one layer paired with a hole in another layer (with respect to the underlying ± 1 integer quantum Hall state), its size is of the same order of the interlayer distance, so could be viewed as a boson in the pseudo-spin channel. In^{52,53,54}, starting from the ESF state, as the distance increases, we studied the instability due to the collapsing of the magneto-roton minimum at q_0 which leads to the formation of the pseudo-spin density wave (PSDW). We showed that a square lattice is the favorite lattice for the PSDW. The interlayer distance in BLQH play a similar role as the pressure in ^4He . Unlike in ^4He where the lattice constant is determined by the pressure, the lattice constant a of the resulting PSDW is completely fixed by the filling factor which is independent of the distance, due to the slight mismatch between the lattice constant a and the instability point $1=q_0$, the resulting PSDW is likely to be an incommensurate solid where the number of sites N_s may not be the same as the number of excitons N even at $T = 0$. As the distance increases further $d_{c1} < d < d_{c2}$, the PSDW lattice constant is still locked at the same value a . Assuming zero-point quantum fluctuations favor vacancies over interstitials, we take $N < N_s$, so there are vacancies n_0 even at $T = 0$ in both top and bottom layers. As argued in⁵², the correlated hopping of vacancies in the active and passive layers in the PSDW state leads to very large and temperature dependent drag consistent with the experimental data. However an excitonic supersolid (ESS) is very unlikely in BLQH. In symmetric electron-hole bilayer system⁵⁵, it was shown in⁵⁶ that it is quite possible that there may a narrow window of ESS where both order parameters are non-vanishing $\langle \dots \rangle \neq 0$; $\langle n_g \rangle \neq 0$ intervening between the ESF and an excitonic normal solid (ENS).

In fermionic systems, it is easy to see the coexistence of CDW and Superconductivity (SC), so "fermionic supersolid" phases are common. For instance, a quasi-two-dimensional system NbSe₂ has a transition to an incommensurate CDW phase at some high temperature T_{CDW} and then a transition to a phase with coexisting CDW and SC order at a lower temperature T_{SC} . The CDW is a pairing in particle-hole channel at $2k_F$, its order parameter is $c_{CDW} = \langle c^\dagger(\mathbf{k})c(\mathbf{k} + \mathbf{Q}) \rangle$ where \mathbf{Q} is the ordering wave vector of the CDW. The SC is a pairing in particle-particle channel also across the Fermi surface. Its order parameter is $c_{SC} = \langle c^\dagger(\mathbf{k})c^\dagger(-\mathbf{k}) \rangle$. Both order parameters are composite order parameters. Different parts of Fermi surface can do the two jobs separately (see, for example,⁵⁷). In contrast to the bosonic SS where there is a density operator n and a complex order parameter, both order parameters c_{CDW} and c_{SC} are complex order parameters. We can see that the formation of a supersolid in a bosonic system has completely different mechanism as shown in this paper, so the QGL theories in the fermionic and bosonic systems could be different to a large extent. It would be interesting to construct a QGL theory to describe the interplay between the two complex order parameters, the properties of the

"fermionic supersolid" (FSS) and the transition from the FSS to the CDW. However, the fermionic excitations near the nodes may be important⁵⁷.

6. Analogy with Type-I and Type-II superconductors

Finally, it may be instructive to make some analogy of Fig.1 and Fig.2 at $T < T_{SF}$ to Type-I and type-II superconductors with the pressure playing the role of the magnetic field H : Fig.1 is similar to Type-I superconductor with SF identified as the Meissner state, the NS as the normal state, the critical pressure p_c identified as the critical magnetic field H_c . Fig.2 is similar to Type-II superconductor with SF identified as the Meissner state, the SS as the mixed vortex lattice state which also breaks both translational order and the global $U(1)$ symmetry, the NS as the normal state, the lower and upper critical pressures p_{c1} and p_{c2} identified as the lower and upper critical magnetic fields H_{c1} and H_{c2} . In superconductors, it is the $\Delta = 0$ to determine Type I and Type II and if the vortex lattice is a stable intermediate state or not as the magnetic field is increased. In Helium 4, it is the sign and strength of the coupling constant g in Eqn.3 to determine the Fig.1 and Fig.2 and if the SS is a stable intermediate state or not as the pressure is increased. So the pressure p and the coupling g in the formation of SS-v play the role of the magnetic field H and Δ in the formation of the mixed state of superconductors. Note that in superconductors, H and Δ are two independent parameters, in ^4He , p and g are also two independent parameters.

XII. CONCLUSIONS

The PSU's experiments renewed the interests in the ^4He system which already had fantastic properties. In this paper, we constructed a two component QGL theory to map out the ^4He phase diagram, analyze carefully the conditions for the existence of the supersolid and study all the phases and phase transitions in a unified view. The only new parameters introduced in the GL theory in this paper is the coupling g and v between the n sector (or normal solid part) and the Δ sector (or the superfluid part) in Eqn.3. We investigated the SS state from both the SF and the NS side and found completely consistent description of the properties of the SS state. Starting from the SF side with increasing the pressure, we developed the theory basing on the two facts (1) there is a roton minimum in the superfluid state (2) the instability to solid formation is driven by the gap diminishing at the roton minimum. By increasing the pressure from the superfluid side, there are two possible scenarios (1) the SF to the C-NS transition in Fig.1 was described by the QGL action Eqn.17 first derived in this paper (2) the SF to the SS transition in Fig.2 is a simultaneous combination of the SDW transition in the n sector driven by the roton condensation at $k_0 = k_r$ and the NS transition in the n sector driven by the divergence in the structure function $k_0 = k_n = k_r$. The superfluid becomes a SS

at lower temperature and a NS at higher temperature (Fig.2). Then we also approached the SS state from the NS side. Depending on the sign and strength of the coupling g between the solid and super uid, we also found two possible scenarios: (1) If $|g|$ is sufficiently small (Fig.4), then the resulting solid at $T = 0; p_{c1} < p < p_{c2}$ is a commensurate normal solid (C-NS). The SS state does not exist as a ground state. However, it may still exist as a metastable state. The QGL action to describe this SF to NS transition in Fig.1 was developed in Sec.IV. (2) If $|g|$ is sufficiently large (Fig.4), the resulting solid at $T = 0; p_{c1} < p < p_{c2}$ is an incommensurate solid with zero point quantum fluctuations generated vacancies if it is negative and interstitials if it is positive (Fig.4). The condensation of the vacancies or interstitials lead to the formation of the SS-v and SS-i respectively. The SS state has lower energy than the NS state at $T = 0$. The $T_{SS,v}$ ($T_{SS,i}$) is an effective measure of the strength of the attractive (repulsive) interaction in the SS-v (SS-i) supersolid. There is no particle-hole symmetry relating $T_{SS,v}$ to $T_{SS,i}$. Our results showed that SS-v is more likely than SS-i. For completeness reason, we discuss both SS-v and SS-i on the same footing although SS-i is unlikely to be relevant to ^4He system. Many physical consequences come out of this single parameter g . Our results on supersolid should be independent of many microscopic details and universal.

Just like the SF is a uniform two-component phase consisting of super uid and normal component at any finite temperature, the SS state is a uniform two-component phase consisting of a super uid density wave (SDW) and a normal solid component even at zero temperature. The SDW in the SS-v coincides with the underlying normal solid. While the SDW in the SS-i state is just a dual lattice to the underlying normal solid. This important fact leads to the key prediction in this paper: the X-ray scattering intensity from the SS-v is similar to that of NS at mean field level, while the X-ray scattering intensity from the SS-i ought to have an additional modulation over that of the NS. The modulation amplitude is proportional to the Non-Classical Rotational-Inertial (NCFI) observed in the torsional oscillator experiments. This prediction is amenable to ongoing X-ray scattering experiments on ^4He at very low temperature. The important effects of Debye-Waller factors on SS-i and SS-v are discussed and will be calculated in future publications²⁹. The NCFI is only weakly anisotropic in the SS phase for hcp lattice. The NS-v (NS-i) to SS-v (SS-i) transition is described by a 3d XY model with much narrower critical regime (Fig.4). The fact that the critical regime of the NS to SS transition is much narrower than the NL to SF transition leads to the two experimentally observable effects of He3 impurities. (1) The He3 impurities decrease the superuid density, but increase the critical temperature transition T_{SS} from the SS to the NS transition. (2) The He3 impurities may smear specific heat jump at $T = T_{SS}$ into a broad peak. Indeed, an excessive specific heat anomaly around 100 mK has been detected in very recent re-

ned experiments in the samples with $x = 0.3 - 3$ ppm at PSU^{12} . By studying all the phases in a unified framework, we conclude there is no SS in hydrogen. We also made comments on several other experiments.

If the supersolid state is responsible for the NCFI observed in PSU 's experiments remains controversial. The GL theory developed in this paper put the competing orders of super uid and solid in the unified framework. It can be used to address many questions raised in PSU 's experiments and other experiments and to make predictions to be tested by future experiments. It can also be applied to study possible supersolid state in other continuous bosonic and electronic systems such as BLQH and electron-hole bilayer system. We suggest that even supersolid may not be realized in ^4He system, it has its own intrinsic, deep and profound scientific interests and impacts and may be realized in other continuous bosonic and fermionic systems.

Acknowledgment

I am deeply indebted to Tom Lubensky for patiently explaining to me the physics of liquid crystal and many insightful and critical comments on the manuscript. I thank P.W. Anderson, M. Chan, T. Clark, M. Ilton Cole, B. Halperin, Jason Ho, D. Huse, J.K. Jain, S. Kivelson, T. Leggett, Mike Ma, G.D. Mahan, S. Sachdev and F.C. Zhang for helpful discussions, A.T. Dorsey for pointing out Ref.²⁵ to me, R.X. Li for technical assistance. I also thank all the participants for many heated and fruitful discussions during the two weeks mini-workshop on supersolid held at KITP at UC Santa Barbara organized by D.M. Ceperley and M. Chan. The research at KITP was supported by the NSF grant No. PHY 99-07949. I also thank the hospitality of Y. Chen, Z. Wang and F.C. Zhang during my visit at Hong Kong University, Yu Lu and Xiang Tao during my visit at Institute for Theoretical Physics in Beijing, China.

APPENDIX A: DISCUSSIONS ON A TOY SUPER SOLID GROUND STATE WAVEFUNCTION

The Ginzburg-Landau theory constructed in the main text is based on order parameters and symmetries. It should hold irrespective many microscopic details such as what is the mechanism responsible for the formation of the supersolid. Despite there are many microscopic calculations for ^4He , constructing a microscopic theory for supersolid is very difficult. In this appendix, I will discuss a well known toy SS wavefunction and clarify a few concepts related to global phase-number uncertainty relation and the role of vacancies or interstitials in the formation of SS. We also clarify the physical meaning of the order parameters n in Eqn.1 and ϕ in Eqn.2. However, because the toy wavefunction may miss some important physics in bulk ^4He systems. For example, due to the very peculiar potential well in the solid ^4He which has a local shallow maximum at the lattice site, the tight bind-

ing model is very crude, Eqn A 1 is built on a rigid lattice, it does not include phonon excitations, so the discussion is very intuitive and crude.

Inside the SF state, because of the strong hard core and long-range correlations between the bare ^4He atom s , the order parameter in Eqn 2 is related to, but should not be taken as the bare ^4He atom annihilation operator, namely, $n(\mathbf{x}) \notin b^{\dagger}(\mathbf{x}) b(\mathbf{x})$. Inside the NS phase, its physical meaning need some explanations. In this section, we discuss the physical meanings of n and n in Eqns. 1, 2, 3 inside the SS state from a toy wavefunction of the SS state.

The toy wavefunction of a supersolid takes the BCS like form

$$\langle \Psi | \hat{S} | S \rangle = \sum_{i=1}^N (u + v b_i^{\dagger}) | \rangle \quad (\text{A } 1)$$

where $u \neq 0$ and $ju^2 + jv^2 = 1$. If setting $u = 0$, the state reduces to a commensurate solid without any vacancies $\langle \Psi | S \rangle = \sum_{i=1}^N b_i^{\dagger} | \rangle$. The commensurate solid (CS) is an exact eigenstate of the boson number operator $N_b = \sum_{i=1}^N n_i$ with the eigenvalue $N_b = N$, so has no chance to become phase ordered. Adding a superfluid component to the CS leads to the SS in Eqn A 1. If setting $v = 0$, then the state reduces to the vacuum state $| \rangle$.

If setting $u = \cos \frac{\pi}{2}$; $v = \sin \frac{\pi}{2} e^{i\phi}$, then Eqn A 1 becomes:

$$\langle \Psi | \hat{S} | S \rangle = \sum_{i=1}^N \left(\cos \frac{\pi}{2} + \sin \frac{\pi}{2} e^{i\phi} b_i^{\dagger} \right) | \rangle \quad (\text{A } 2)$$

where ϕ .

By construction, the state has the translational order with the average boson density $\langle n_i \rangle = ju^2 = \sin^2 = 2$, so the average vacancy density is $ju^2 = \cos^2 = 2$. It is easy to see that $\langle \Psi | S \rangle$ also has the ODLRO with $\langle b_i \rangle = u v = \frac{1}{2} \sin e^{i\phi}$, so $\langle \Psi | S \rangle$ is indeed a supersolid state. The angle ϕ controls the magnitude, while the phase ϕ controls the phase of the condensation. Defining $b_{k=0} = \frac{1}{\sqrt{N}} \sum_{i=1}^N b_i$ which satisfy the boson commutation relation $[b_0, b_0^{\dagger}] = 1$, the boson operator at zero momentum is $n_0 = b_{k=0}^{\dagger} b_{k=0}$, the total number of bosons at the zero momentum state is $N_0 = \langle \Psi | \hat{S} | S \rangle = \frac{N}{4} \sin^2 =$

$N_b \cos^2 = 2 < N_b = N \sin^2 = 2 < N$. At integer filling $n = 1$, the superfluid state $\langle \Psi | S \rangle = \frac{1}{\sqrt{N!}} (b_{k=0}^{\dagger})^N | \rangle$, then $N_0 = \langle \Psi | \hat{S} | S \rangle = N_b = N$. Obviously, this SF state is not included in the family in the Eqn A 1.

A supersolid state $\langle \Psi | S | N_b \rangle$ with N_b bosons is given by:

$$\langle \Psi | S | N_b \rangle = \sum_{i=1}^{Z_2} \frac{d}{2} e^{i\pi b_i} \langle \Psi | S | \rangle \quad (\text{A } 3)$$

where the total boson number N_b and the global phase ϕ are two Hermitian conjugate variables satisfying the commutation relation: $[N_b, \phi] = i\pi$. It leads to the uncertainty relation $N_b \phi = 1$.

It is easy to see $\langle N_b \rangle = \frac{N}{2} \langle jv^2 \rangle = N \sin^2 = 2$; $N_b = \sqrt{\langle N_b^2 \rangle - \langle N_b \rangle^2} = \sqrt{\frac{N}{2} \langle jv^2 \rangle} = \sqrt{N} \sin \phi$; $N_b = \langle N_b \rangle = \frac{1}{\sqrt{N}} \langle ju \rangle = \frac{1}{\sqrt{N}} \langle jv \rangle = \frac{1}{\sqrt{N}} \langle jv \rangle = 2$. If $\phi \neq \pi$, the absolute boson number fluctuation $\langle N_b^2 \rangle - \langle N_b \rangle^2$ is quite large, so ϕ could be quite small, so one can get a phase ordered state. On the other hand, the relative boson number fluctuation $\langle N_b - \langle N_b \rangle \rangle = \frac{1}{\sqrt{N}}$ is quite small, so one can still measure the average boson number accurately. The first quantization form of the Eqn A 3 can be derived by the same method used in²².

Because in the SS state, there is a global phase ordering in ϕ , so its conjugate variable is the total number of particles N_b as shown in Eqn A 3. The local tunneling or exchanging processes stressed in⁴ may not cause the total number fluctuations, therefore may not cause the global phase ordering leading to the supersolid phase. The discussions in this appendix is at most instructive. It is known that state Eqn A 1 may not describe the ground state of the solid ^4He Hamiltonian well, but what it implies is that if the vacancies in an incommensurate solid could lead to the formation of a supersolid. In this indeed happens, in the GL theory constructed for SS-v in the main text, the bosons are represented by $n(\mathbf{x})$, while the vacancies are represented by $b(\mathbf{x})$. A toy wavefunction for SS-i is not written down so far, because the interstitials are moving between lattice sites. In the SS-i, the bosons are represented by $n(\mathbf{x})$, while the interstitials are represented by $b(\mathbf{x})$.

¹ C. N. Yang, Rev. Mod. Phys. 34, 694 (1962).

² A. Andreev and I. Lifshitz, Sov. Phys. JETP 29, 1107 (1969).

³ G. V. Chester, Phys. Rev. A 2, 256 (1970).

⁴ A. J. Leggett, Phys. Rev. Lett. 25, 1543 (1970).

⁵ W. M. Saslow, Phys. Rev. Lett. 36, 1151?1154 (1976).

⁶ For review of NCFI in atomic gases, see Franco Dalfovo, Stefano Giorgini, Lev P. Pitaevskii and Sandro Stringari, Rev. Mod. Phys. 71, 463?512 (1999); Anthony J. Leggett, Rev. Mod. Phys. 73, 307?356 (2001).

⁷ E. Kim and M. H. W. Chan, Nature 427, 225 ? 227 (15 Jan 2004).

⁸ E. Kim and M. H. W. Chan, Science 24 September 2004; 305: 1941?1944.

⁹ A. C. Clark and M. H. W. Chan, J. Low Temp. Phys. 138, 853 (2005).

¹⁰ E. Kim, M. H. W. Chan, Phys. Rev. Lett. 97, 115302 (2006).

¹¹ A. C. Clark, X. Lin, M. H. W. Chan, cond-mat/0610240.

¹² M. H. W. Chan, private communication and to be submitted.

ted.

¹³ D . M . Ceperley, B . Bernu, Phys. Rev. Lett. 93, 155303 (2004); N . P rokof'ev, B . Svistunov, Phys. Rev. Lett. 94, 155302 (2005); D . E . Galli, M . Rossi, L . Reatto, Phys. Rev. B 71, 140506(R) (2005); Evgeni Burovski, Evgeni Kozik, Anatoly Kuklov, Nikolay Prokof'ev, Boris Svistunov, Phys. Rev. Lett., vol. 94, p. 165301 (2005). M . Boninsegni, A . B . Kuklov, L . Pollet, N . V . Prokof'ev, B . V . Svistunov, and M . Troyer, Phys. Rev. Lett. 97, 080401 (2006).

¹⁴ W . M . Saslow, Phys. Rev. B 71, 092502 (2005); N . K um ar, cond-mat/0507553; G . B askaran, cond-mat/0505160; Xi D ai, M . ichael M a, Fu-Chun Zhang, Phys. Rev. B 72, 132504 (2005); Hui Zhai, Yong-Shi W u, J. Stat. Mech. P 07003 (2005).

¹⁵ A . T . D orsey, P . M . G oldbart, J . Toner, Phys. Rev. Lett. 96, 055301 (2006).

¹⁶ P . W . A nderson, W . F . B rinkman, D avid A . H use, Science 18 Nov. 2005; 310: 1164-1166.

¹⁷ Jinwu Ye, Phys. Rev. Lett. 97, 125302 (2006).

¹⁸ Ann Sophie C . R ittner, John D . Reppy, Phys. Rev. Lett. 97, 165301 (2006).

¹⁹ James D ay, T . H eman and John B eamish, Phys. Rev. Lett., vol 95, 035301 (2005).

²⁰ I . A . Todoshchenko, H . A lles, J . Bueno, H . J . Junes, A . Ya . Parshin, and V . T sepelin, Phys. Rev. Lett. 97, 165302 (2006)

²¹ I thank Tom Lubensky for discussions leading to the fact that there should be this n sector in addition to the σ sector.

²² Gun Sang Jeon and Jinwu Ye, Phys. Rev. B 71, 035348 (2005) .

²³ Jinwu Ye, Density wave states in super uid, cond-mat/0512480.

²⁴ T . Schneider and C . P . Enz, Phys. Rev. Lett. 27, 1186 (1971); Y ves P om eau and Sergio R ica , Phys. Rev. Lett. 72, 2426 (1994).

²⁵ P . N ozieres, J. Low . Temp . Phys. 137, 45 (2004).

²⁶ Guenter Ahlers , Phys. Rev. A 3, 696C 716 (1971); Dennis S . G reyw all and Guenter Ahlers , Phys. Rev. A 7, 2145C 2162 (1973).

²⁷ It can be easily shown that including both the spin waves and vortex excitations in \downarrow will not change the following results.

²⁸ For discussions on Classical Lifshitz Point (CLP) and their applications in nem atic to sm ectic-A and -C transitions in liquid crystal, see the wonderful book by P . M . Chaikin and T . C . Lubensky, Principles of Condensed Matter Physics, Cambridge university press,1995.

²⁹ Jinwu Ye, unpublished.

³⁰ I thank Tom Lubensky for discussions leading to the fact that the \downarrow phase factor is important and may lead to super uid Goldstone mode.

³¹ R . Shankar, Rev. Mod. Phys. 66, 129?192 (1994).

³² S . A . B razovskii, JETP 41, 85 (1975).

³³ Feynman originally conceived the roton as drifting vortex loop. But this point of view is very controversial. If taking this view , then the roton condensation can be considered as vortex loop condensation.

³⁴ In 2 + 1 dimensional Bilayer quantum Hall system s, the magnetoroton dispersion relation is $\omega^2 = q^2(a - bq + cq^2)$ due to long-range Coulomb interaction. See⁵².

³⁵ B . A . Fraass, P . R . G ranfors, and R . O . Simmons, Phys. Rev. B 39, 124C 131 (1989). C . A . Burns and E . D . Isaacs, Phys. Rev. B 55, 5767C 5771 (1997).

³⁶ I thank Tom Lubensky for this observation.

³⁷ J . E . H o man et al. Science 295, 466 (2002).

³⁸ S . R . W hite and D . J . Scalapino, Phys. Rev. Lett. 80, 1272 (1998).

³⁹ The core energy is always much smaller than the super flow energy even for large size of vortex core.

⁴⁰ John M . G oodkind, Phys. Rev. Lett. 89, 095301 (2002).

⁴¹ K . S . Liu and M . E . Fisher, Jour of Low Temp . Phys. 10, 655, (1973).

⁴² Jinwu Ye, Quantum phase transitions from solids to supersolids in bipartite lattices. cond-mat/0503113.

⁴³ Jinwu Ye, Supersolids and solids to supersolids transitions in frustrated lattices. cond-mat/0612009.

⁴⁴ P . A . C rowell and J . D . R eppy, Phys. Rev. Lett. 70, 3291C 3294 (1993); Phys. Rev. B 53, 2701C 2718 (1996).

⁴⁵ P . W . A nderson; Science 235, 1196 (1987).

⁴⁶ H . W . E chert and K . K ortmann, Phys. Rev. B 70, 125410 (2004).

⁴⁷ M . G reiner, O . M andel, T . E sslinger, T . W . H ansch, T . B loch, N ature 415, 39-44 (2002).

⁴⁸ G . C . B atrounil et al, Phys. Rev. Lett. 74, 2527 (1995); ibid, 84, 1599 (2000).

⁴⁹ P inakiSengupta, et al, Phys. Rev. Lett. 94, 207202 (2005).

⁵⁰ Ganpathy M urthy, Daniel A rovas, A ssia A uerbach, Phys. Rev. B 55, 3104 (1997).

⁵¹ For a review, see S . M . G irvin and A . H . M acdonald, in Perspectives in Quantum Hall e ects, edited by S . D as Sam a and A . P inczuk (W iley, New York, 1997).

⁵² Jinwu Ye, Quantum Phase transitions in bilayer quantum Hall system s at total filling factor $\tau = 1$, cond-mat/0606639.

⁵³ Jinwu Ye, Fractional charges and quantum phase transitions in imbalanced bilayer quantum Hall system s. Phys. Rev. Lett 97, 236803 (2006).

⁵⁴ Jinwu Ye, Mutual Composite Fermion and Composite Boson approaches to balanced and imbalanced bilayer quantum Hall system s: an electronic analogy of Helium 4 system , cond-mat/0310512.

⁵⁵ L . V . Butov, C . W . Lai, A . L . Ivanov, A . C . G ossard, D . S . Chem la, L . V . Butov, A . C . G ossard, D . S . Chem la, N ature 418, 751 - 754 (15 Aug 2002). D . S noke, S . D enev, Y . L ii, L . P fei er, K . W est, N ature 418, 754 - 757 (15 Aug 2002). D avid S noke, N ature 443, 403 - 404 (28 Sep 2006). C . W . Lai, J . Zoch, A . C . G ossard, and D . S . Chem la, Science 23 January 2004 303: 503-506. U . S ivan, P . M . S olomon, and H . S htrikman, Phys. Rev. Lett. 68, 1196C 1199 (1992). S . D e Pablo*, F . R apisarda2, and G aetano S enatore1, Phys. Rev. Lett. 88, 206401 (2002).

⁵⁶ Jinwu Ye, unpublished.

⁵⁷ A . H . C astro N eto, Phys. Rev. Lett, 86, 4382 (2001).